



UNIVERSIDAD
DE GRANADA

PHYSICS AND SPACE SCIENCES

DOCTORAL THESIS

**Interfacial characterization of heavy
naphthenic bitumen for paving**

Author:

Felipe II GUERRERO BARBA

Supervisors:

Dr. Miguel A.

RODRÍGUEZ-VALVERDE

Dr. Miguel A.

CABRERIZO-VÍLCHEZ

Granada - April 28, 2017

Editor: Universidad de Granada. Tesis Doctorales
Aur: Felipe II Guerrero Barba
ISBN: 978-84-9163-558-1
URI: <http://hdl.handle.net/10481/48432>

El Doctorando Felipe II Guerrero Barba y los directores de la tesis Dr. Miguel A. Rodríguez-Valverde y Dr. Miguel A. Cabrerizo-Vílchez, garantizamos, al firmar esta tesis doctoral, que el trabajo ha sido realizado por el doctorando bajo la dirección de los directores de la tesis y hasta donde nuestro conocimiento alcanza, en la realización del trabajo, se han respetado los derechos de otros autores a ser citados, cuando se han utilizado sus resultados o publicaciones en la realización del trabajo.

Granada, April 28, 2017

Director de la Tesis

Director de la Tesis

Doctorando

M.A. Rodríguez-Valverde

M.A. Cabrerizo-Vílchez

F. Guerrero Barba

Contents

Acknowledgements	1
Motivation	3
1 Materials and methods	11
1.1 Bitumens	11
1.1.1 Bitumen-in-water dispersions	12
1.1.2 Bitumen films	13
1.1.3 Calcareous aggregates	13
1.2 Experimental techniques	13
1.2.1 Contact angle hysteresis	13
1.2.2 Contact angle measurement	14
1.2.3 Surface energy measurement	15
1.2.4 Interfacial tension measurement	15

1.2.5	High temperature Goniometer	17
1.2.6	Electrophoretic mobility measurement	19
2	Interfacial energy of heavy naphthenic bitumen in aqueous medium	21
2.1	Results and discussion	22
2.1.1	Electrical state of naphthenic bitumen in aqueous medium	22
2.1.2	Surface energy of naphthenic bitumen	22
2.1.3	Contact angle hysteresis of naphthenic bitumen films	23
2.1.4	Interfacial energy of naphthenic bitumen in aqueous medium	24
2.2	Conclusions	25
3	Interfacial tension of heavy naphthenic bitumen in water at high temperature: effect of pH and calcium ions	29
3.1	Results and discussion	30
3.1.1	Bitumen surface tension	30
3.1.2	Effect of pH on the bitumen contact angle	31
3.1.3	Electrical state of bitumen-in-water dispersion	31
3.1.4	Bitumen-water interfacial tension	32
3.1.5	Effect of pH on the bitumen-water interfacial tension	33
3.1.6	Effect of calcium ions on the bitumen-water interfacial tension	34
3.2	Conclusions	35
4	Bitumen spreading on calcareous aggregates at high temperatures	37
4.1	Results and discussion	38
4.1.1	Bitumen surface tension	38
4.1.2	Bitumen spreading	38
4.1.3	Bitumen films	42
4.1.4	Cross-sectioned calcareous aggregates	42

4.2	Conclusions	43
5	Summary and Conclusions	45
A	Supplementary data	49
A.1	High-temperature chamber for interfacial/surface tension measurements of heavy bitumen	49
A.2	Stability of bitumen-water interfacial tension	49
A.3	Rigid skin	51
	Bibliography	53

Acknowledgements

This thesis was supported by “Ministerio Español de Economía y Competitividad” (project MAT2014-60615-R) and the “Junta de Andalucía” (project P12-FQM-1443). F. Guerrero and his supervisors are grateful to the Biocolloid and Fluid Physics Group (ref. PAI-FQM115) of the University of Granada (Spain). Special thanks go to Dr. Didier Lesueur for his fruitful discussions during the conceptual stages of this work.



Motivation

History

Bitumen, also known as Asphalt in America is a black and highly viscous liquid or semi-solid. It may be found in natural deposits or may be a refined product. The word asphaltum is also used and it is derived from the Ancient Greek *ásphaltos*. The words asphalt and bitumen are used interchangeably to mean both natural and manufactured forms of the same substance. Bitumen/Asphalt refers to the refined residue from the distillation process of selected crude oils. The use of bitumen as an adhesive dates of the fifth millennium BC. The Sumerians (first known civilization) used natural bitumen deposits to manufacture hunting tools. Several millennia later, when the first civilizations were conformed, the uses of bitumen were widely extended. Hot asphalt was used as mortar in the walls of Babylon. In the river Euphrates at Babylon, the 1 km long Euphrates Tunnel was constructed of burnt bricks covered with bitumen as a waterproofing agent. Bitumen was used by ancient Egyptians to embalm mummies.

Ubadis developed small boats by using bitumen as cement, to travel by the Persian Gulf. This way, they became in the first documented mariners of history. Centuries later, Muslim doctors prescribed bitumen to treat lesions and skin diseases. However, not all ancient civilizations used bitumen. For example, in Mesopotamia, they did not know how to control bitumen flammability, this led the Acadians to call bitumen as naptu, precursor of the Arabic word naft (napht).

On the other side of the world, bitumen was also used, especially as when it was formed on large lake-shaped surfaces. Some of the largest in the world are: Pitch Lake in Trinidad and

Tobago, Rancho La Brea in Los Angeles California and Guanoco in Venezuela. In pre-Hispanic Mexico bitumen was a material used both in a practical and religious way. Nowadays, bitumen is known as Chapopote. This word comes from the Náhuatl words *chiáhuatl* (which means fat) and *pochtli* (smoke). The use of bitumen has a history of at least two thousand years, mostly in the area of the Gulf of Mexico, where this natural material has been used as fuel, medicine, waterproofing, coating of tools for hunting and utensils, for painting for decoration, etc. It was also an important part in the manufacture of balls used in the classic ball game (1). It was also mixed with a yellow ointment extracted from the insects, this became into a mild and odorous mixture called *tzictli* from which the chewing gum was derived, this mixture was chewed for using as toothpaste and dental bleach (2). Due to its special characteristics that make it a unique substance on earth, in which, about 95% of the world production is destined to the construction of roads (3).

Most people are not familiar with bitumen, however all of us know the black carpet that we use every day. Most of the road surfaces are black due to the agent used as a binder to fabricate roads, this is bitumen, which is mixed with aggregates of crushed rocks. Nevertheless, the roads surface may also be grey. This is in the case that the binding agent used is the Portland cement.

Road paving

Bitumen at room temperature it is a black visco-elastic solid, and as the temperature increases it becomes a viscous liquid. The bitumen has adhesive and waterproofing properties, which makes the material particularly suitable for bonding aggregates. To prepare the asphalt mixture, the bitumen must be heated to a sufficiently high temperature to achieve a suitable viscosity that facilitates the spread over the dry and preheated aggregates. At present, the main challenge of the road paving industry is to strengthen its sustainable development. Asphalt roads are made from mineral aggregates and a bitumen binder heated to temperatures between 160 and 200 °C. Bituminous mixtures for road paving are usually fabricated at high temperatures and they are transported to the site where bitumen is going to be deposited and compacted at high temperatures. Bitumen is extended and compacted at about 100 °C. When bitumen temperature gets low, it becomes more viscous and the mixture hardens (4). In the last decades, research devoted to bituminous mixtures has been oriented to lower temperatures. In hot mixtures, the aggregates are dried at high temperatures, before they mix with hot bitumen. Warm mixtures are fabricated by mixing the aggregates with their natural humidity with the hot binder.

Bitumen is a colloidal system (3), its composition is a complex mixture of many organic components. Its continuous phase is composed by maltenes and constitute the fraction of asphalt which is soluble in n-alkane solvent such as pentane and n-heptane. Maltenes are mainly composed by three structural groups, saturates, aromatics and resins. The discontinuous phase is composed

by asphaltenes (highly polar) that are formed by heavy aromatic molecules forming micelles (5). Bitumen properties strongly depend on their origin (see Figure 1) due to variation of the its components proportion like Saturates, Asphaltenes, Resines, Aromatics (SARA) or acidity index (mg KOH/g crude needed for neutralization). Worldwide crude oil acid numbers vary less than 0.01 to as high of 3 (6).

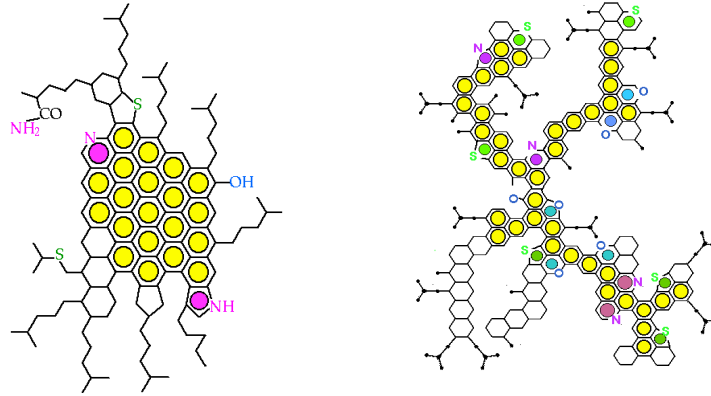


Figure 1: Molecules of maya (left) and venezuelan (right) bitumen.

Since bitumen needs to be handled and applied hot, paving industry has progressively developed bitumen emulsions, giving rise to an alternative approach in which bitumen is finely dispersed in water. The benefits of cold paving technologies are their respect for the environment by reducing energy costs (the aggregates do not dry and the working temperature of the binder is lower) as well as the emissions of fumes in the mixing plant and during the spreading. Moreover emulsions of micron particle (5-10 μm) allow to improve the coating of the aggregates and the mechanical properties of the cold mixtures (7). The performance of bitumen emulsions can be evaluated through several conventional properties; however, these properties depend on the formulation of the emulsion, composition of bitumen and the emulsification process

Bituminous slurries for surface treatments to improve surface texture or pavements sealing are mixtures made at room temperature with a binder (bituminous emulsion), aggregates, water and eventually, mineral powder (filler), the consistency of which is suitable for its implementation and can be applied in one or several layers (see Figure2). The main mechanisms of breaking emulsions are the strong absorption of water from aggregates, pH rise and cation release. Here the breaking of emulsion (destabilization) is caused by varying the pH (acid to basic), either by evaporation or by the addition of cement (hygroscopic agent and with high calcium content). However, the breaking of emulsions of Nynäs bitumen (Laguna Laguna, Venezuela), of naphthenic nature, is not so straightforward.

Microsurfacing is similar to slurry seal. It consists of the application of a mixture of water,



Figure 2: Application of bituminous slurry on mineral aggregates.

bitumen emulsion, aggregates and chemical additives to an existing pavement surface. This technique is a good alternative to give preventive maintenance and repair roads. It is an economic and efficient technique and it is increasingly being used in road paving industry (8).

Interfacial response of bitumen: state-of-the-art

The interfacial systematic study of bitumen dates back to the beginning of the last century, when Nellensteyn and Roodenburg were able to measure the contact angle of various bitumens to determine the bitumen surface tension for temperatures between 0 and 100 °C (9). Several studies have also been made with the purpose of evaluating the adhesion work of bitumen on the aggregates. Moraes et al. (10) estimated the bitumen cohesion and adhesion by measuring the surface energy with the sessile drop technique. The experiments were conducted at room temperature. To explore adhesion and wetting kinetics of bitumen emulsions on mineral surfaces, Ziyani et al (11) studied 4 mineral substrates (gneiss, diorite, limestone and quartzite) and 3 different emulsions with the sessile drop technique and a commercial tensiometer (DSA 100, Krüss GmbH). They prepared the bitumen emulsions and then deposited a sessile drop on the mineral substrates at room temperature. The interfacial tension was also measured. Khan et al (12) characterized the free surface energy for both systems, minerals and binders, by means of contact angle measurements. The binders used in those experiments were unmodified Nynäs bitumen, with three penetration grades: 160/220, 70/100 and 50/70. The sessile drop technique was used with the commercial tensiometer (DSA 100, Krüss GmbH). H.R. Fischer et al (13) covered with bitumen different minerals (mica, calcite) and glass. The interaction of bitumen with the limestone, mica and glass was studied with AFM. They found no significant difference between macroscopic and microscopic contact angles.

The tension at the bitumen-water interface is the primary surface property of the emulsified droplet. It represents the energy required to create new interfacial surface area and, as such, is a measure of the deformability of emulsion droplets. Further, it is the two-dimensional analogue to

pressure and can be considered a state variable from a thermodynamics perspective. That is, at a set temperature and pressure, an interface between two immiscible liquids should possess a unique equilibrium tension value. This equilibrium tension may, however, be sensitive to compositional effects at the interface such as those arising from surfactant adsorption.

Using the spinning drop technique (homemade technique), M. Di Lorenzo et al. (14) measured the equilibrium interfacial tension of bitumen at 30, 60 and 75 °C. With this technique, they obtained more accurate results for low and high tension values. However, this technique does not work for almost equal densities between phases. To study the effects on the interfacial tension of different commercial emulsifiers, Chaverot et al (15) measured interfacial tension of 7 different bitumens at high temperatures (90 -140 °C) using the pendant drop technique immersed in water. They used a high pressure chamber. They found that the interfacial tension depends strongly on the measuring time and it does not depend of the surfactants used.

Measuring interfacial tension between bitumen and aqueous surfactant solutions can be difficult task because of these systems usually have densities that are closely matched, which it may have a significant impact on measurement accuracy. In addition, bitumen has also extremely high viscosity which restricts the application of these techniques. The measurements with viscous liquids, like bitumen, are always difficult to carry out due to problems with handling the liquid, injection of a liquid sample of the required volume into the instrument, low-velocity liquid flow, and long-time viscous effects during deformation of the interface.

Aims of thesis

The understanding of the (un)stability mechanisms of bitumen-in-water emulsions is of paramount importance in the "cold" technology of road construction (4). Bitumen emulsions for road paving are designed to break when they are spread on gravels. The breaking process becomes especially critical in time-dependent applications such as in slurry seals and microsurfacing. In these applications, the balance between slurry fluidity and re-opening to traffic is imposed. The kinetics of coalescence of bitumen particles will condition the rate of the cohesion built-up (16). Thereby, the formulation of bituminous slurries is optimized on purpose for each work site.

The nature of bitumen plays a relevant role in bituminous slurries because the interfacial and electrical behaviors of bitumen-in-water emulsions are modulated by the naturally-occurring surfactants of bitumen (3) during the coalescence process (17). Hence, the interfacial properties of bitumen become significant during the breaking stage (18), rather than during the emulsification process. It is well established that naphthenic bitumen may be spontaneously dispersed in basic water without extra emulsifier (19). Bitumen in aqueous medium usually reveals ionizable surface groups onto its surface (20). These groups, mainly carboxylic acids and amines, further act

as surface active species activated by the medium pH (19). In this scenario, the native surfactants present in naphthenic bitumen (with a high content of naphthenic acids) are greatly active. Thereby, interfacial tension enables to examine meaningfully the behavior of naphthenic bitumen in aqueous media (15).

For breaking (phase separation) of bitumen emulsions, after coalescence, two bitumen drops diffuse into each other by interfacial relaxation ruled by a competition between interfacial tension and viscous dissipation. When coalescence happens, if the relaxation time is sufficiently high compared to the coalescence kinetics, a network of coalesced particles can form before the relaxation is completed which leads to the formation of a gel (21) rather than a solid phase completely separated from water. In general, emulsion coalescence is accelerated when the salinity increases in water phase. It is known that emulsion destabilization is faster for divalent ions than for monovalent ions but calcium ions are further specific for bitumen. After adding a destabilizing agent (lime, cement or calcareous fillers) to a bitumen emulsion, as happens in microsurfacing, calcium naphthenates are formed from the specific adsorption at the bitumen-water interface between the free calcium ions (from the added calcium carbonate) of the aqueous medium and the surface carboxylate groups of bitumen. This produces lower interfacial elasticity (22). Boucard et al. (23) found that acidic bitumen accelerates the coalescence kinetics of the emulsion although its relaxation were slow due to the bitumen viscosity and composition. Otherwise, several authors have reported the effects of pH on crude oil/water systems. Strassner (24) found that Venezuelan crude oil emulsions inverted in oil/water at high pH ($\text{pH} \approx 10.5$). Goldzal (25) observed a high stability in emulsions at high pH values in acidic crude emulsions.

Several methods for measuring the interfacial tension of bitumen in water have been reported in literature (14, 26–29). However, the heavy bitumen-water system has mainly two drawbacks: a highly viscous phase at room temperature (low fluidity, high interfacial relaxation) and a vanishing density difference. In certain methods, such as the Du Noüy ring and the Wilhelmy plate, it is necessary to decrease bitumen viscosity at room temperature by dilution in toluene or benzene. Since bitumen can readily flow at a high temperature, several authors used the pendant drop technique for interfacial tension measurements of bitumen-water systems (30, 31). The techniques based on drop shape may become inaccurate for systems of nearly matched densities. Besides, bitumen drop equilibration may become so slow that no steady state is reached during the time period studied because the endogenous surfactants must diffuse through the bitumen bulk and adsorb at the interface. Moran et al. (32) used the micron-scale tensiometry as alternative route.

For most liquid-fluid interfaces (isotropic phases), due to the fast molecules diffusion between phases (i.e. chemical equilibrium), interfacial tension numerically coincides with the respective specific interfacial energy. This does not happen at common solid-liquid interfaces due to the absence of diffusion equilibrium. Hence, a solid-liquid-vapour system can be mechanically stable but far from the thermodynamic equilibrium. Despite of the experimental inaccessibility of interfacial

energies associated to solid phases, contact angle appears as a simple, useful and sensitive tool for quantifying the interfacial energy of bitumen films in contact with pure water or aqueous surfactant solutions (33–35). Moreover, contact angle titration may reveal the acid-base properties of bitumen (36).

A good adhesion between bitumen and aggregate is fundamental for the production of high quality asphalt mixtures. Bitumen-aggregate adhesion should be quantified at a practical level to select the materials and to assess stripping potential (37). The methodology followed for quantifying bitumen-aggregate adhesion should examine the formation of physical, chemical, and/or mechanical bonds across the bitumen-aggregate interface. However, the quantification of the physico-chemical bond between bitumen and aggregate under realistic conditions is a nontrivial task (38–40).

Thermodynamic adhesion work between bitumen and mineral aggregate depends on the equilibrium values of bitumen surface tension and bitumen-aggregate contact angle. The sessile drop method offers a fast and convenient way to probe the surface energetics of asphalt bitumen binders and mineral aggregates (18). Otherwise, the physico-chemical bond between bitumen and aggregates should be measured at temperatures closer to the temperature of the asphalt mixtures produced at mixing plants (150-190°C) (41). The aggregates coated with bitumen in a hot mix plant are subjected to very high temperatures just prior to mixing. This enables the removal of moisture from the aggregate surface. In other respects, migration of endogenous surfactants of bitumen towards the interface is favoured at high temperatures. Bitumen/substrate and bitumen emulsion/substrate adhesion is strongly dependent on the surface properties of the materials. In particular, it is reported that surface energy contributes more to the total adhesion than mechanical and chemical adhesion (42)

In this thesis, measurements of contact angle, surface tension and interfacial tension were performed to evaluate important parameters such as adhesion, and, surface energy, to monitor the spreading at high temperature of bitumen sessile drops. We used the sessile drop and pendant drop methods in our laboratories. For the experiments of interfacial tension, we designed ad hoc an apparatus to form pendant drops (maximum 180 μ l) of bitumen at high temperature (maximum 100 °C) in water solutions. We also designed a high-temperature goniometer to measure the contact angle of liquid bitumen on mineral substrate.

In chapter 1 we describe the instruments and methods used in this thesis.

The aim of chapter 2 is the evaluation of the interfacial energy of heavy naphthenic bitumen in water at different values of pH and at room temperature. We propose a new methodology based on the measurement of the bitumen surface tension at high temperature, the equilibrium contact angle of buffered water on heat-casted films of bitumen and the estimation of the bitumen-water interfacial energy at room temperature using the Young equation (43). Our strategy enables us to

avoid the use of approaches for surface energy calculation, such as the polar-disperse components of surface tension (44) and the equation of state (33, 45).

In chapter 3 we intend to understand the behavior of naphthenic bitumen in water due to the activation of endogenous surfactants. We measured the bitumen-water interfacial tension at high temperature for different pH values and the "underwater" wettability of bitumen films. We also examined the effect of calcium ions on the interfacial tension and electrical state of bitumen.

Finally, in chapter 4, we examined the physicochemical interactions between bitumen and aggregate during bitumen spreading at high temperature. We monitored the spreading of sessile drops of liquid bitumen deposited on polished limestone aggregates. We selected limestone sheets due to their importance in road paving and because calcite is very chemically active (38). We studied two bitumens with different interfacial, rheological, and chemical properties: naphthenic bitumen and asphaltic bitumen.

Materials and methods

1.1 Bitumens

In this study, we used bitumen Nynäs 80/100 (Venezuela), usually devoted to slurry seal applications for road paving. This type of bitumen is highly viscous (21) and reveals a high acid content (acid number 3.16 mg KOH/g) The values of density at different temperatures were kindly provided by Nynäs, density 1.020 g/cm³ at 25°C and 0.962 g/cm³ at 120°C. The natural surfactants of bitumen are activated through the pH in aqueous medium. For this reason, the pH was actively controlled during the experiments of chapter2 with buffer solutions of low ionic strength ($\leq 15\text{mM}$) (46).

The naphthenic bitumen has a high content of naphthenic acids that act as native surfactants in aqueous media at alkaline conditions (pH>10). To compare the interfacial behaviour of the naphthenic bitumen, we also studied an asphaltic bitumen produced in Mexico (provided by Repsol, penetration grade 150/200 without further modification). We used the density values of bitumen at different temperatures (from 90 to 160°C) kindly provided by Nynäs ($\rho(\text{g}/\text{cm}^3) = -0.0006T(^{\circ}\text{C}) + 1.034$). The density of bitumen was slightly higher than the density of pure water (less of 3.5%) as illustrated in Figure 5.1. Penetration bitumen, predominantly asphaltic (3) and is the most widely used for hot mixes. This bitumen used in this work is less viscous

and less acidic than the naphthenic one. The density of the penetration bitumen in terms of temperature was reported by Repsol.

1.1.1 Bitumen-in-water dispersions

To prepare the bitumen in-water dispersions (see Figure 1.1), the naphthenic bitumen was heated at 250 °C and the buffered water at 90 °C. Then 4g was poured into warm water buffered at different pH values, without added emulsifier. To overcome the interfacial tension forces, the bitumen water suspension was sheared with a stirrer (BOECO OSD-20) at 1500 rpm for 45 min. After vigorously shaking, the fine dispersion of bitumen was just spontaneous at pH=12. This pointed out that the formation of bitumen droplets occurred by capillary break-up at pH =12 due to that the bitumen-water interfacial tension reached a minimum value. Next, we left to rest the suspension for a period of 3 to 5 h for setting the larger particles. Subsequently, we removed the supernatant and the deposits. This procedure was conducted for different pH. The bitumen dispersion obtained was highly polydisperse. The bitumen dispersion at pH12 was the unique stable (2.2% w/w) as illustrated in Figure 1.1. Due to the high concentration, we diluted it at 0.011% w/w. The mean diameter of bitumen particles, measured with an ALV-NIBS High Performance Particle Sizer was $(2.5 \pm 2.0) \mu\text{m}$ and the maximum content of bitumen dispersed was 2.2% (w/w). Despite of that the bitumen density is very close to the water density, the settling of the dispersion occurred overnight due to the large size of the bitumen particles. However, the particles were readily redispersed in bulk by shaking. We were unable to reproduce the spontaneous emulsification with paraffinic and asphaltic bitumens.



Figure 1.1: Dispersion of naphthenic bitumen in water at pH 12.

1.1.2 Bitumen films

A bitumen film reasonably behaves as a smooth solid surface (33). Glass cover slips (18-20 mm diameter) were treated with a pulsed laser beam (Nd:YAG, Laser E-20 SHG II, Rofin) to form a 0.5-1mm diameter hole at the center. The function of this hole is explained in Section 1.2.2. The bitumen was initially heated (150°C). The hot bitumen was carefully laid on the cover slips, which were previously heated in a hot plate at 90°C for 1 h. Before bitumen coating, the hole of the cover slips was protected with a steel needle. The slips covered with bitumen were placed in an oven at 90°C for one hour. The smoothness of the film was ensured once the bitumen homogeneously spread on the cover slips (the roughness values were lower than 2 nm measured with AFM over an area of $5 \times 5 \mu\text{m}^2$). In order to allow the arrangement of the asphaltenes and other bitumen compounds, the films were cooled inside the oven once turned off. The final film thickness was roughly 1 mm. Finally, the bitumen films were stored in closed Petri dishes at room temperature for a minimum of 24h before contact angle measurement.

1.1.3 Calcareous aggregates

We employed polished limestone sheets (containing at least 90% of calcite and 98% of carbonates (47)) as substrates to deposit sessile drops of liquid bitumen. The preparation of aggregate sheets is described in the work of (48). The substrates dimensions were $(1.5 - 2) \times (2.5 - 3) \text{ cm}^2$. The roughness values for three different samples were $R_a = 1.5$ and $R_q = 2.4 \mu\text{m}$, measured by White Light Confocal Microscopy (WLCM, PI μ Sensofar) over different scanned areas ($5.1 \times 5.6 \text{ mm}^2$, $9.8 \times 4.6 \text{ mm}^2$ and $14.1 \times 10.1 \text{ mm}^2$).

To obtain cross-sectioned samples of the mineral substrates covered by the solid bitumen, after drop spreading, we entirely immersed each mineral substrate in an epoxy resin (EpoxyCure 20-8130-032). Once the resin was hardened, the piece was cut with a mechanical saw. This way, the cutting process was easier and no residue was observed at the bitumen/limestone interface.

1.2 Experimental techniques

1.2.1 Contact angle hysteresis

For a solid-liquid-vapour system at thermodynamic equilibrium, the Young equation relates the interfacial energies γ_{ij} associated to each interface to the contact angle θ (see Figure 1.2):

$$\cos \theta = \frac{\gamma_{SV} - \gamma_{SL}}{\gamma_{LV}} \quad (1.1)$$

where the subscripts, L, V and S refer to the liquid of the drop, the vapour in the surrounding medium and the solid surface, respectively. It should be noted that this solid surface is assumed to be perfectly smooth, isotropic, rigid and chemically inert. However, on moderately rigid solids and at experimental time scales, a mechanical equilibrium configuration is usually realized at the three-phase contact line rather than a global thermodynamic equilibrium state (49). Due to this, the contact angle θ in the Young equation is experimentally inaccessible. Besides, the observable contact angle can take multiple values due to the non-ideal features of nearly all solid surfaces.

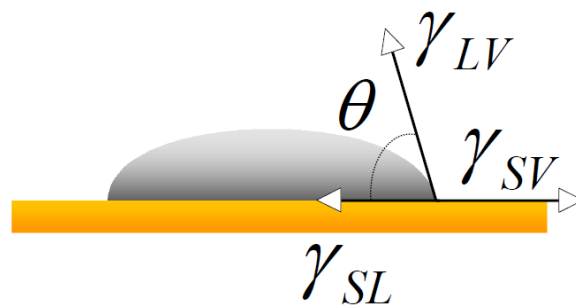


Figure 1.2: Contact angle: The angle θ forms the solid surface with the tangent to the liquid surface at the triple point of contact.

1.2.2 Contact angle measurement

It is well established to estimate the equilibrium contact angle as the arithmetic mean of the advancing contact angle and the receding contact angle (50). With this purpose, contact angle hysteresis measurements were performed at room temperature using the low-rate dynamic contact angle technique. This technique is based on the growing and shrinking of a sessile drop by adding and removing water respectively, through a hole made in the substrate. The set-up and methodology are described in detail elsewhere (51). We performed the experiments with sessile drops of MilliQ water buffered at different pH values (in the range 2-12) on the bitumen films prepared in Section 1.1.2.

To study the "underwater" wettability properties of the bitumen films, we used the captive bubble method (52). This way, the film is always immersed in water. This enables to evaluate hydrated bitumen. Moving a sessile drop over a previously wetted surface (receding mode, as opposed to a previously dry surface (advancing mode)), can induce surface mobility and reorientation, liquid penetration, or local swelling. This may be further enhanced in "underwater" conditions like in the captive bubble method. We checked that the water surface tension was stable for each

experiment and its value was independent of the pH value. In our technique, a growing/shrinking bubble was formed against the film. The bubble volume was varied through the hole drilled to the film with a 250 μl syringe connected to a micro injector (PSD3, Hamilton) (53). The advancing and receding contact angles were averaged over the values of contact angle observed when the bubble contact line was steadily moving against the film. In these experiments, the pH of the aqueous phase was varied between 2 and 12 by adding dropwise *NaOH* or *HCl* (Sigma Aldrich) up to reach the desired pH. This had no significant effect on the final ionic strength of the aqueous solution.

1.2.3 Surface energy measurement

We used the pendant drop method for measuring the surface tension of bitumen at high temperature (see Figure 1.3). We used the conventional set-up of the pendant drop technique, although we further designed an aluminum open chamber with two windows (32.5x13 mm²) and a metallic conical syringe with a tip of 1.5-mm diameter (see Figure 1.4). The syringe enabled to dispense hot bitumen by turning a steel screw within the syringe instead of moving a plunger. The chamber was heated with a thermocouple. Unlike the Du Noüy ring and Wilhelmy plate methods, in the pendant drop there is no solid surface (ring, plate...) interacting closely with bitumen. This fact minimized the eventual pollution. At a high temperature, we filled the dispensing device, next we fixed it to the warmed chamber and finally, we formed a bitumen drop at the tip of the dispensing device in a glass cuvette inserted inside the chamber. Once the drop was formed, we began to acquire a sequence of side-view images of the drop upon diffuse back illumination. As reported in literature (26, 54), we reasonably assumed the linear dependence of surface tension on temperature, over a wide range. This way, we estimated the surface energy of solid bitumen as the value of surface tension extrapolated to room temperature.

1.2.4 Interfacial tension measurement

We designed ad-hoc an instrument to measure interfacial/surface tension of bitumen by using the pendant drop method (15, 55). The apparatus consisted of a high-temperature chamber, a dispensing device and an optical system (see Figure 1.5). Once the bitumen drop was formed, we began to acquire a sequence of side-view images of the drop upon diffuse back illumination. The image acquisition and processing were performed with a software developed in our laboratories. This software fits the experimental drop profiles, extracted from the drop digital images, to the solution of the Young-Laplace equation, and it provides the drop volume, interfacial tension and interfacial area (56).

To perform interfacial tension measurements at high temperature, we built an aluminium close



Figure 1.3: Bitumen pendant drop formed at high temperatures.

chamber of 9.2 cm in height, 9.6 cm in length and 2 cm in width, with two circular apertures of 2.6 cm of diameter, with glasses of 1 cm of thickness and 3.8 cm of diameter. Each glass window was sealed with two PTFE rings and fixed with six stainless steel screws (7.6 cm of length and 6 mm of diameter, see Figure A1 in Supplementary Data). The interfacial tension measurements performed at high temperature (close to the boiling point of water) during longer periods of time might produce water evaporation. To mitigate it, we strongly fitted and locked all mobile components of the chamber.

The temperature of the chamber was controlled with a Peltier PT100 resistance (max. temperature 200 °C). We used as dispensing device a stainless steel hollow cylinder with a conical tip of 2.5 mm diameter and an internal stainless steel screw, which enables the drop formation inside the chamber. The main components of the optical system were a LED source and a CMOS video camera (PixeLINK®, Canada) attached to a microscope objective (0.60 lens magnification, Edmund Optics, USA). To mitigate eventual vibrations during the measurement and to maintain stable pendant drops, the stage of the equipment was supported with rubber pads on a table.

Before each experiment, the dispensing device and chamber were thoroughly cleaned with xylene (LeycoChem LEYDE), next rinsed with Milli-Q water and allowed to dry in air. The syringe and bitumen were heated separately up to 150 °C. Then, the syringe was filled with hot bitumen and rapidly attached to the chamber. The system was allowed to equilibrate at the set temperature before forming the pendant drop. For bitumen-water measurements, the chamber was previously filled with the aqueous phase fixed in pH and calcium ion concentration. A scale calibration was conducted from the images of a graticule placed inside the chamber with water.

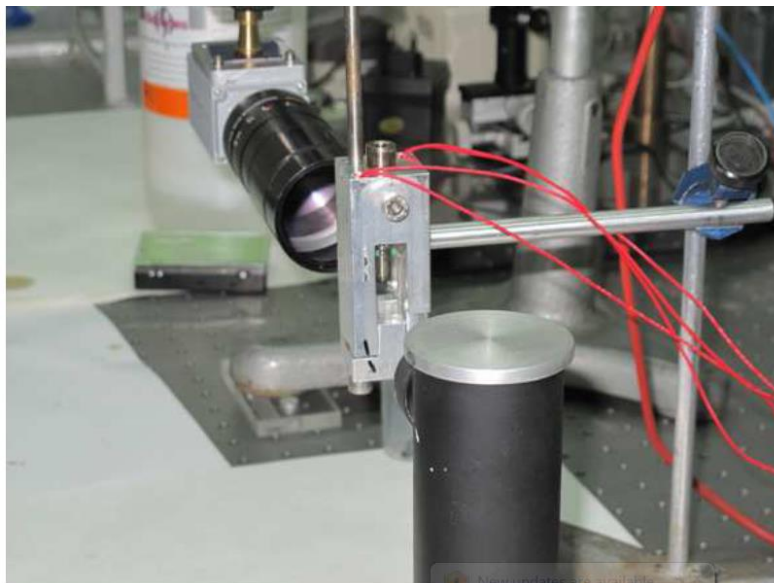


Figure 1.4: First set-up to measuring bitumen pendant drop at high temperatures.

The difference of mass density between bitumen and water determines the drop orientation: pendant or captive drop, ruled by the balance between gravity force and hydrostatics. Since our bitumen was slightly denser than water (see Figure 5.1), the pendant drop configuration was reproduced. We were able to form stable pendant drops with large volumes due to the small density difference between bitumen and water over the temperature range explored. The sphere (circle, in two dimensions) is the zero gravity shape for pendant and sessile drops/bubbles. The circular drop profile is also obtained when the densities of both liquids agree. The fitting algorithm of drop profiles processes satisfactorily gravity-distorted drops but does not work accurately with small volume drops or spherical drops. There is a critical shape parameter above which the drop is considered well deformed (56). In the experiments of interfacial tension in terms of calcium ions, we used calcium chloride ($CaCl_2$, Sigma Aldrich)

1.2.5 High temperature Goniometer

We used the sessile drop method to monitor bitumen spreading over the limestone substrates. With this purpose, we designed a high temperature goniometer. The substrate was placed into an aluminum chamber ($75 \times 50 \times 15\text{mm}^3$) with two lateral windows ($70 \times 15\text{mm}^2$) (see Figure 1.6). The chamber was heated at a temperature controlled with a thermocouple (Eurotherm 2132). The temperature can be varied within the range 70-120°C. A brass syringe with a conical tip of 1.5mm diameter and a with internal thread, enabled to dispense liquid bitumen by turning a steel screw within the syringe acting as a plunger. At high temperature, we filled the syringe and then we fixed it to the top of the previously warmed chamber. Next, we deposited a bitumen

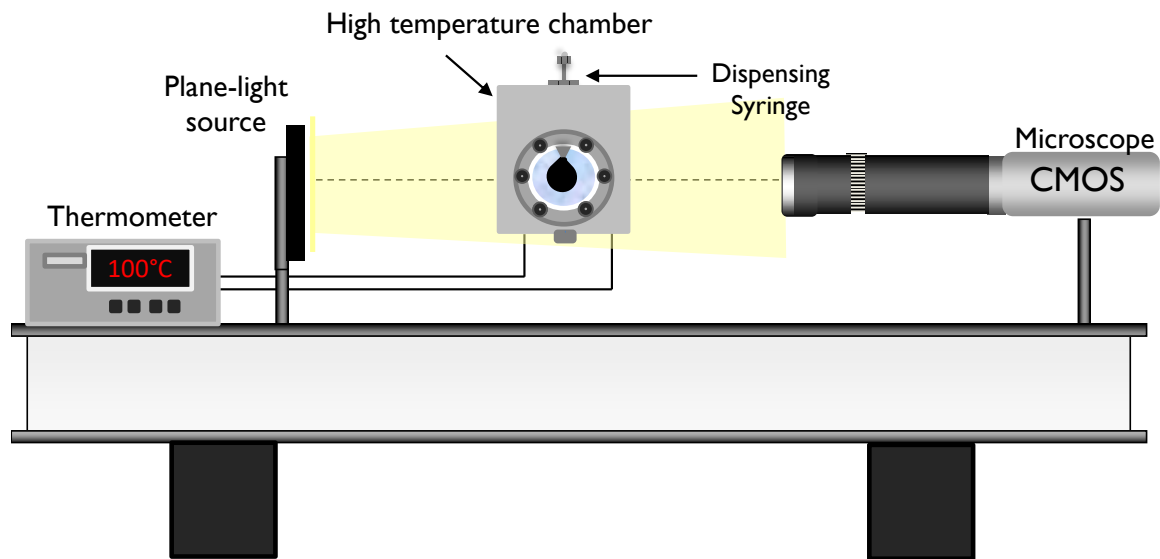


Figure 1.5: Layout of the experimental setup for the interfacial/surface tension measurements at high temperature.

sessile drop ($25\text{-}40\mu\text{l}$) on the hot substrate. The drop was back illuminated using a plane and homogeneous light source. Side-view images of the drop were acquired with a CCD camera (PixelLink PL-A741). Drop profiles were analyzed with the Axisymmetric Drop Shape Analysis-Profile (ADSA-P). This technique allows to measure simultaneously the liquid surface tension (γ), drop volume (V), contact radius (r_c) and contact angle (θ) (57). The minimum value of contact angle measured was about $15\text{-}20^\circ$ because the ADSA-P algorithm is numerically unstable for low contact angles.

We performed several drop depositions for each temperature on different limestone substrates. However, due to the time elapsed between the drop deposition and image focusing, the origin of timescale was different for each run. The kinetic nature of the experiment and the high variability of the limestone substrates avoided any statistically meaningful averaging. We deposited just one drop per each substrate because after spreading, a bitumen thin film significantly covered the substrate.

Since the surface tension of the naphthenic and asphaltic bitumens was reasonably constant from the beginning of each experiment of drop spreading (not shown), the bitumen surface tension for each temperature was averaged over time during one experiment. This way, the equilibrium surface tension reflected the actual interaction between the bitumen and mineral during the drop spreading. To validate the reliability of the high temperature goniometer, the surface tension of the naphthenic bitumen was further measured with the pendant drop method described by Guerrero-Barba et al (58). With this method, we averaged the values of equilibrium surface tension measured in three different experiments because there was no disturbing solid-liquid interface.

The temperature (of each element) was continuously monitored with a small probe inside the chamber. The temperature of the chamber, substrate and air, measured separately, was stable after 500s (see Figure 1.7), once it reached the target temperature. This procedure assures the thermal equilibrium between bitumen and aggregate during the spreading, unlike the procedures used in literature based on the melting of initially solid bitumen on hot aggregates (59).

The film dimensions (thickness, h_f and contact radius, r_f) were measured from the last image captured at the end of each experiment (after 14 – 25h, accordingly). The contact angle (θ_f) of the bitumen film (pancake-like drop) was estimated from the expression:

$$\theta_f = 2 \arcsin \frac{h_f}{2l_0} \quad (1.2)$$

known the corresponding capillary length (l_0) for each bitumen and temperature.

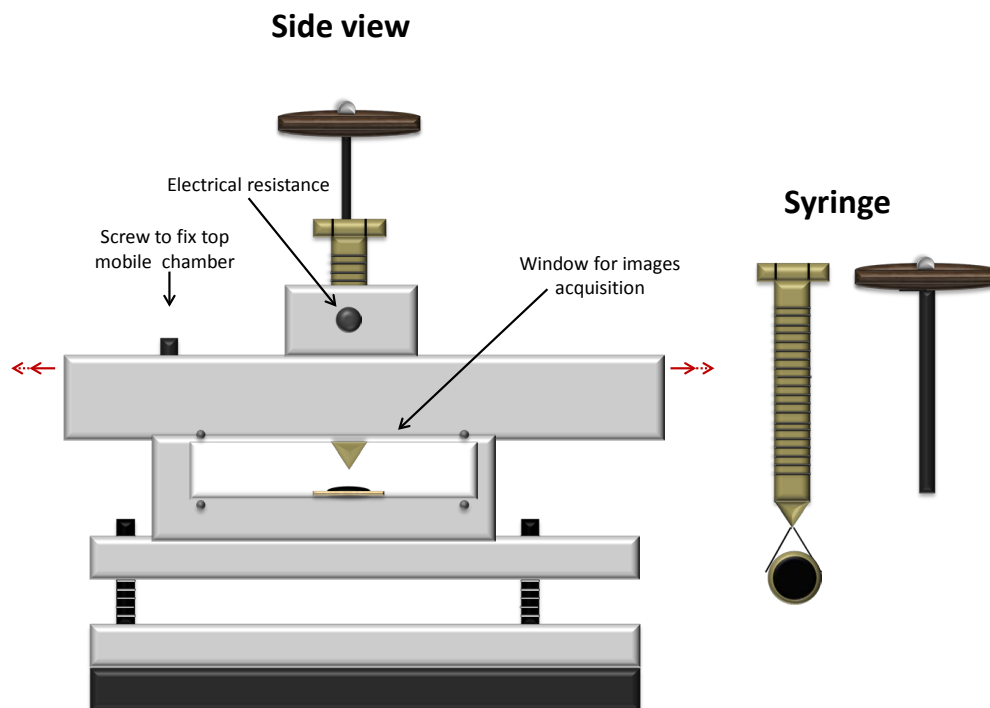


Figure 1.6: Layout of the chamber used for the deposition of bitumen sessile drops at high temperature. The arrows indicate the moving top part of the chamber.

1.2.6 Electrophoretic mobility measurement

To examine the electrical state of the (surfactant-free) bitumen-in-water dispersion (prepared in Section 1.1.1), we measured the electrophoretic mobility with a Zeta PALS (Brookhaven Instru-

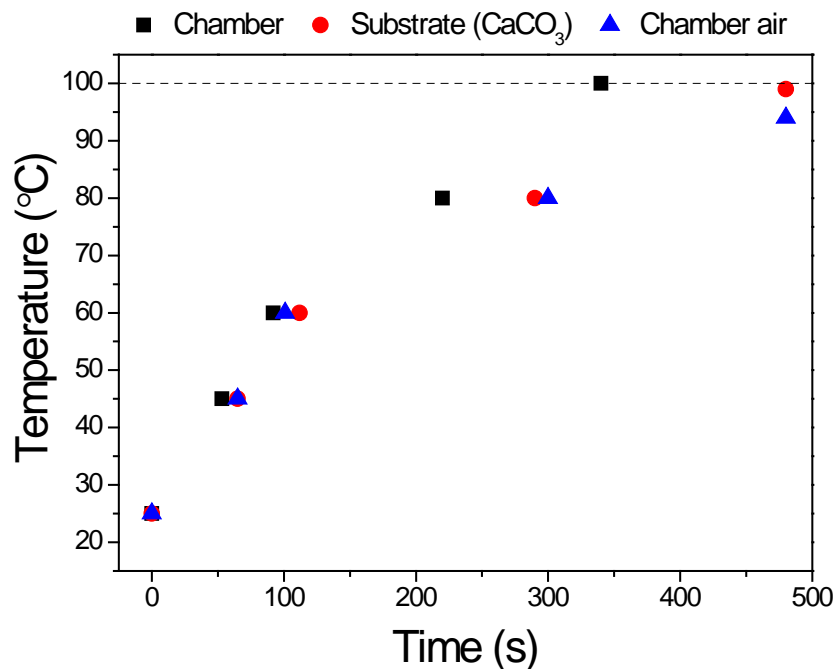


Figure 1.7: Temperature inside the chamber and its parts in terms of time. The thermocouple was fixed to 100°C.

ments) at room temperature. We diluted the bitumen-in-water dispersions prepared up to 0.011% w/w in buffer solutions of low ionic strength ($\leq 15\text{mM}$) to fix the pH of the medium. The dispersion pH was varied from pH 2 to 13. We conducted three runs for each pH value with different samples.

To evaluate the calcium ion effect, we used calcium nitrate ($\text{Ca}(\text{NO}_3)_2$) from 0.05 up to 50 mM. The electrophoretic mobility of the dispersion at acidic conditions (pH 2-6) was rapidly measured (max. two minutes including the sample preparation) to avoid the coagulation of the sample.

Interfacial energy of heavy naphthenic bitumen in aqueous medium

In this chapter, we propose an approach for predicting the interfacial energy of bitumen in aqueous media based on contact angle hysteresis measurements. We measured the surface tension of naphthenic bitumen at high temperature with the pendant drop method. We estimated the surface energy of bitumen as the value of surface tension extrapolated to room temperature. The acid-base properties of naphthenic bitumen films were investigated by contact angle titration with buffered water. Due to the occurrence of contact angle hysteresis, we performed advancing-receding contact angle measurements on bitumen films at different values of pH with the low-rate dynamic contact angle technique. We observed that the receding angle was dependent on pH. Instead, advancing contact angle just reflected the nature of bitumen in dry conditions. We chose the average contact angle of advancing and receding contact angles as an estimate of the thermodynamically meaningful contact angle. Finally, the bitumen-water interfacial energy at room temperature was calculated using the Young equation. The low interfacial energy of bitumen at high pH confirmed the existence of native surfactants.

2.1 Results and discussion

2.1.1 Electrical state of naphthenic bitumen in aqueous medium

The results of electrophoretic mobility in terms of pH are shown in Fig. 2.1. Each point in the graph represents the average of three runs performed over three different samples. The electrophoretic mobility values agree in magnitude with those reported in literature (34). As expected, the dissociated anionic surfactants (mainly carboxyl groups) dominate the bitumen surface above pH 4. The bitumen particles revealed the maximum (negative) electrical charge at pH 12. The unexpected increase of electrophoretic mobility at pH 13 points out to the incipient coalescence of the dispersion. The isoelectric point ($pH_{iso}=3$) comes from the balance between the effect of the basic (amines) and acidic functional groups of the naphthenic bitumen (3). It is known that the strong acidic groups of the naphthenic bitumen are able to produce a decrease of the isoelectric point regarding paraffinic bitumen.

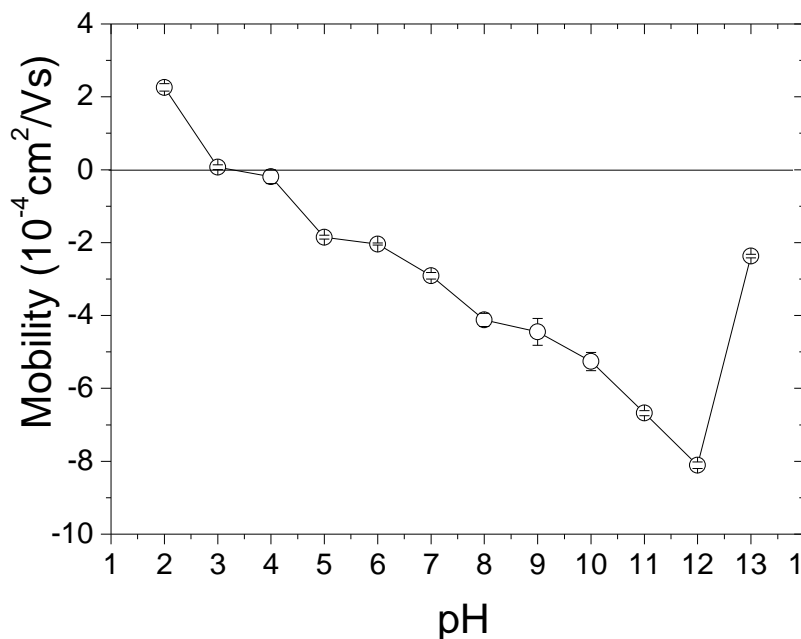


Figure 2.1: Electrophoretic mobility of naphthenic bitumen-in-water dispersion in terms of the medium pH. Bitumen revealed the isoelectric point at pH 3 and a maximum electrical state at pH=12.

2.1.2 Surface energy of naphthenic bitumen

In Fig. 2.2, we plot the surface tension of bitumen in terms of temperature. For each temperature, we selected the stable value of surface tension reached before falling the bitumen drop. Above

150°C, the bitumen surface tension was so low that it was not possible to form a static pendant drop at the tip of our dispensing device. The linear dependence of surface tension on temperature is confirmed. By extrapolation of the surface tension data to 25°C, the surface energy of (solid) bitumen was $31.7 \pm 0.5 \text{ mJ/m}^2$. This value reasonably agrees with the value reported in literature (26, 54) and with the bitumen surface energy computed from static captive bubble measurements (34). This agreement points out to that the bitumen surface energy at room temperature is not significantly sensitive to the migration of polar bitumen components and to the partial oxidation in air produced during surface tension measurements at high temperature, as suggested by Hefer et al. (60).

F.II Guerrero-Barba et al./Fuel 112 (2013) 45–49

47

interacting closely with bitu-
l pollution. At a high temper-
ice, next we fixed it to the
rmed a bitumen drop at the
ss cuvette inserted inside the
d, we began to acquire a se-
p upon diffuse back illumina-
s of bitumen at different
ndly provided by Nynäs ($\rho(g/$
nsity of bitumen was slightly
r (less of 3.5%). As reported in
ned the linear dependence of
r a wide range. This way, we
bitumen as the value of sur-
temperature.

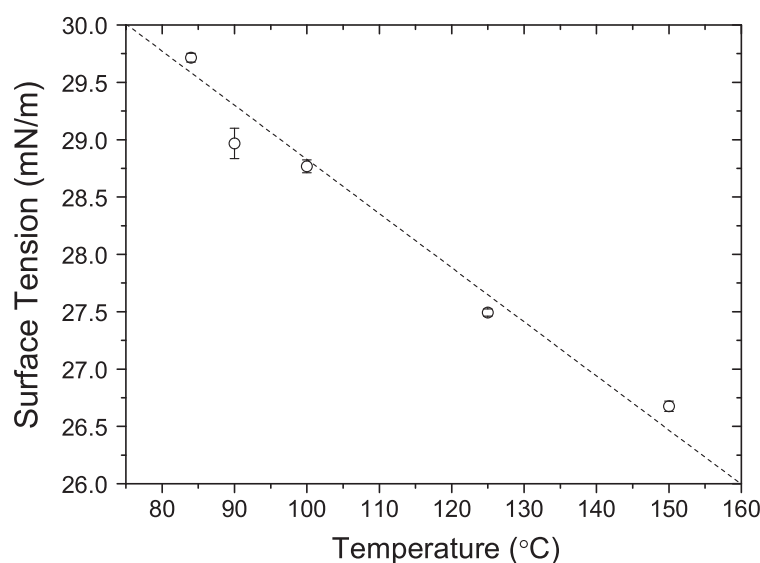


Figure 2.2: Surface tension of naphthenic bitumen in terms of the temperature. By extrapolation to 25°C the surface energy of (solid) bitumen was $31.7 \pm 0.5 \text{ mJ/m}^2$.

thermodynamic equilibrium, the
facial energies γ_{ij} associated to

with sessile drops of MilliQ water buffered at different pH values (in the range 2–12) on the bitumen films prepared in Section 2.2.

2.1.3 (1) Contact angle hysteresis of naphthenic bitumen films

3. Results and discussion

to the liquid of the drop, the
nd the solid surface, respec-
olid surface is assumed to be
d chemically inert. However,
experimental time scales, the
n is usually realized at the
a global thermodynamic equi-
contact angle θ in the Young
ible. Besides, the contact angle
s due to the non-ideal features
l established to estimate the
ometric mean of the advancing
ct angle [26]. With this pur-
urements were performed at
e dynamic contact angle tech-
e growing and shrinking of a
g water respectively, through
-up and methodology are de-
performed the experiments

in Fig. 2.3, we plot the advancing and average contact angles in terms of water pH. We observed how the advancing contact angle remained constant as the medium pH. In agreement with Jacobasch et al. (67), advancing angle is not adequately sensitive to characterize the acidic character of bitumen films because it must reflect the nature of bitumen in dry conditions. The electrophoretic mobility values agreed in magnitude with those reported in literature (4). Instead, the advancing angle was sensitive to changes in pH. During the entire experiment of low-rate dynamic contact angle (few minutes), the surface tension of the buffered water agreed with the value of pure water. The traces of light beige or transparent were detected in water. In consequence, we observed no macroscopic deformation of the bitumen films due to the unresolved acids. The isoelectric point ($pH_{iso} = 3$) comes from the balance between the effect of the basic (amines) and acidic functional groups of the naphthenic bitumen [3]. It is known that the strong acidic groups of the naphthenic bitumen are able to produce a decrease of the isoelectric point regarding paraffinic bitumen.

3.2. Surface energy of naphthenic bitumen

vertical component of the water surface tension (35).

It is well established that advancing contact angles reveal the low-surface energy domains of a solid surface (e.g. apolar surface groups) whereas receding angles are closely related to the high-surface energy domains (e.g. polar surface groups). The main ionizable groups onto the bitumen surface are amino and carboxyl (20), although the surface density of carboxyl groups in naphthenic bitumen is much greater than the density of amino groups. Moreover, the carboxyl group, because of the two oxygens, can form hydrogen bonds with five water molecules and is, therefore, more hydrophilic than the amino group.

Bitumen is negatively charged above pH 3, close to the pK_a value of the carboxyl group (see Fig. 2.1). Bitumen is electrically uncharged when the carboxyl groups are barely half ionized and counterbalance the surface density of amino groups. Within the pH range (3, 8), receding contact angle increased as the pH due to the zwitterionic behavior of bitumen: the carboxyl groups are un-protonated and the amino groups protonated. Above pH 8, close to the pK_a of the amino group, the receding contact decreased up to pH 12, where the carboxylic groups are entirely ionized.

We computed the average contact angle between the advancing and receding angles for the pH range 2-12. This value was used as estimate of thermodynamically meaningful contact angle (50), which appears in the Young equation (1.1).

2.1.4 Interfacial energy of naphthenic bitumen in aqueous medium

Finally, we estimated the bitumen-water equilibrium interfacial energy from the Young equation (1.1) at different pH values (see Fig. 2.4). We used the value of bitumen surface energy obtained in Section 2.1.2, the values of average contact angle calculated in Section 2.1.3 and the surface tension of pure water at room temperature. The changes in interfacial energy with pH revealed the activity of native acids and bases of bitumen. The values obtained are in good agreement with the values reported in literature for the naphthenic bitumen from Venezuela (19, 31, 62). As expected, the lowering interfacial energy is closely related to the density of carboxyl functional groups at the bitumen-water interface. The complete ionization of these natural surfactants (at pH 12) minimized the interfacial energy (up to a few mJ/m^2) and maximized the electrical state (see Fig. 2.1). We also found that the presence of calcium ions (from 0.05 to 5 mM) in the water drops at pH= 12 increased the equilibrium contact angle (see Figure 2.5) and as a result, the interfacial energy of bitumen also increased, in agreement with other authors (29). The calcium ions fixed the carboxyl groups onto the bitumen interface by specific binding, and in consequence the interfacial activity of bitumen was arrested.

Our methodology does not enable to capture the dynamic behavior of interfacial tension caused

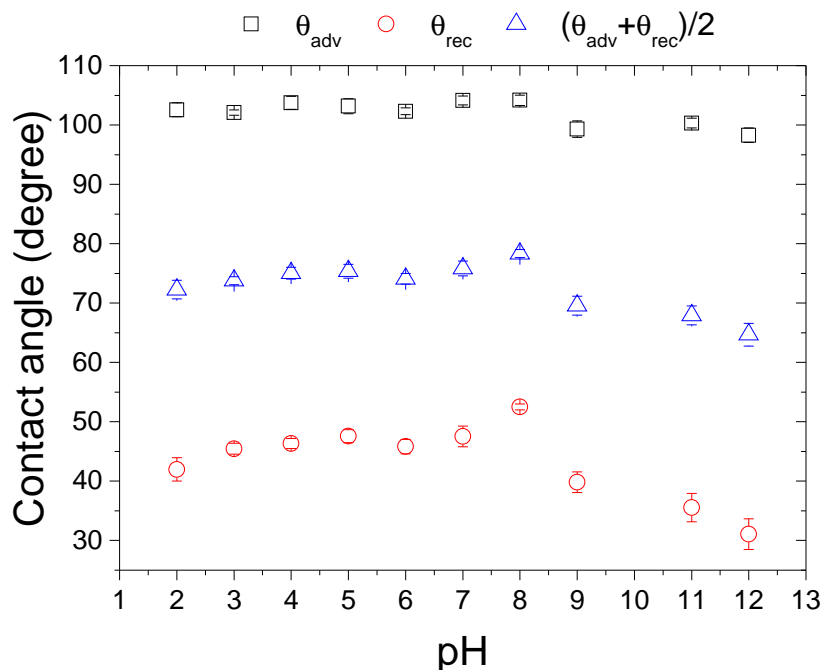


Figure 2.3: Advancing, receding and average contact angles of buffered water on smooth films of naphthenic bitumen in terms of the pH. We observe how the receding contact angle reached a maximum value at pH= 8, close to the pK_a of the amino group, and a minimum value at pH= 12 where the carboxylic groups are entirely ionized.

by the diffusion of natural surfactants from the bitumen bulk towards the bitumen-water interface. Instead, the interfacial energy obtained from Eq. (1.1) is, at least, related to a mechanical equilibrium configuration of the bitumen-water system at room temperature. However, we are able to monitor the wettability response of bitumen films to sudden changes of pH in the water drop. This would be very representative for bituminous slurry surfacing where the interfacial dynamics of bitumen becomes critical at rapidly increasing values of medium pH.

2.2 Conclusions

The methodology introduced in this chapter enables the evaluation of the bitumen-water equilibrium interfacial energy at room temperature. Unlike the pendant drop method for bitumen-water interfacial tension measurements at high temperature, our strategy is appropriate for systems with vanishing density differences and with a very slow interfacial relaxation (high viscosity, low interfacial tension). Further, we avoided the bitumen dilution (eventual traces of solvent), the use of probe liquids for contact angle measurements (mutual solubility with bitumen) and of theories for surface energy calculation (polar-disperse components of surface tension, equation of state). The low-rate dynamic contact angle technique was successfully applied to raw (solvent-

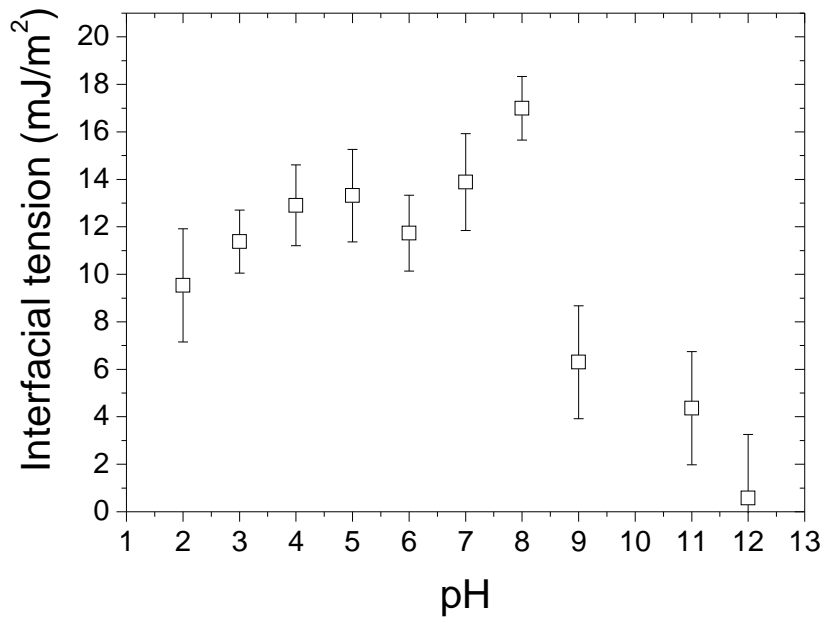


Figure 2.4: Interfacial energy of naphthenic bitumen calculated from Eq. (1.1) in terms of the medium pH. We observe a maximum value at pH=8 and a minimum value at pH=12.

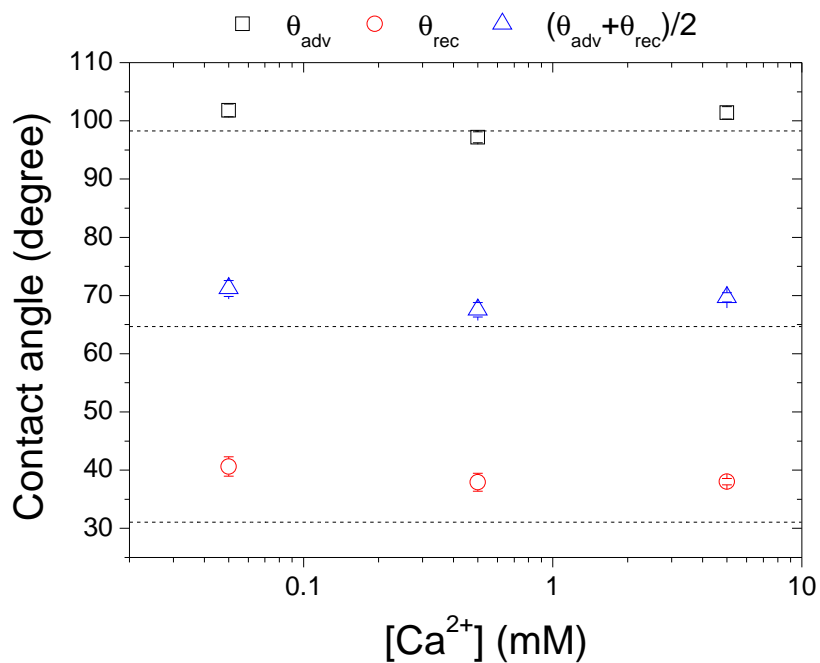


Figure 2.5: Contact angle of water drops of pH = 12 in presence of calcium ions (from 0.05 to 5 mM)

free) bitumen films for contact angle hysteresis measurements. Receding contact angles revealed the acid-base properties of naphthenic bitumen. We estimated the bitumen interfacial energy in aqueous medium from the Young equation using the average contact angle of the advancing and receding contact angles for different pH values. The naphthenic bitumen showed high interfacial activity in alkaline aqueous medium (above pH 9) with maximum electrical state and minimum interfacial energy at pH=12. This confirms the self-emulsifiable character of naphthenic bitumen in basic water.

Interfacial tension of heavy naphthenic bitumen in water at high temperature: effect of pH and calcium ions

The aim of this chapter is the understanding of the interfacial activity of the natural surfactants present in heavy naphthenic bitumen. We present an experimental study to evaluate the effect of the pH and calcium ions on the naphthenic bitumen-water interface from the interfacial tension at high temperature (pendant drop method) and bitumen wettability at room temperature (under hydrated conditions). We designed ad hoc a high temperature tensiometer for viscous bitumen. We performed advancing-receding contact angle measurements on bitumen films at different values of pH with the captive bubble method. To assess the electrical state of surfactant-free bitumen dispersions in water, we measured the electrophoretic mobility in function of pH and content of calcium ions. The changes in the interfacial tension and wettability in terms of pH revealed the complex interfacial activity of naphthenic bitumen. The presence of calcium ions decreased the unsigned electrical charge of bitumen and, at alkaline conditions, it increased the bitumen interfacial tension because the interfacial layers of calcium naphthenates instead of pure naphthenic acids.

3.1 Results and discussion

3.1.1 Bitumen surface tension

The surface tension of naphthenic bitumen was measured over the temperature range from 70 to 100 °C. The surface tension values were stable for 800 s approximately, after the pendant drop was formed (see Figure A.2). To compare the surface activity of naphthenic bitumen, we also studied asphaltic bitumen (63). The equilibrium values of surface tension for the naphthenic and asphaltic bitumens as a function of temperature are plotted in Figure 3.1. In both systems the surface tension linearly decreases as the temperature over the range of temperatures explored. Increasing temperature enhances the thermal motion of bitumen molecules that reduce their cohesive forces. The surface tension of the naphthenic bitumen is slightly lower than the asphaltic bitumen. Some surface-active light molecules migrate from the bulk towards the bitumen surface (in air). However, the surface activity of these unionized native surfactants is very similar for both bitumens.

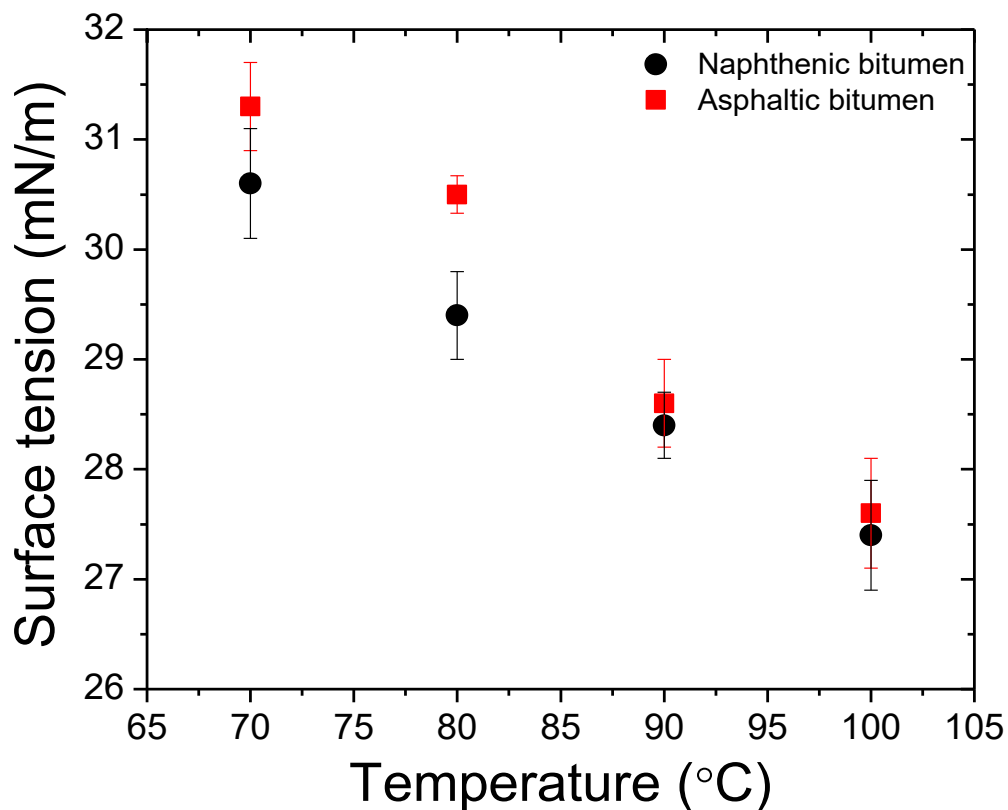


Figure 3.1: Surface tension of naphthenic and asphaltic bitumen in terms of temperature.

3.1.2 Effect of pH on the bitumen contact angle

In Table 3.1, we collect the values of advancing contact angle (ACA) and receding contact angle (RCA) of naphthenic and asphaltic bitumen films for pH2 and pH12. The ACA values for each bitumen were similar, regardless of the pH value. The ACA obtained values are in good agreement with reported in the literature for different bitumens (34). The wettability (ACA and RCA) of naphthenic bitumen films with MilliQ water (pH \approx 5-6) and acid water (pH2) was very similar. However, the bitumen wettability was different at pH12, because RCA was lower than at pH2 for both bitumens. Bitumen reveals more high-energy surface domains at pH12 due to the ionization of the surface carboxylic groups. The values of RCA for naphthenic bitumen were lower than for asphaltic bitumen. This points out to a greater density of carboxylic groups correlated with the high bitumen acidity.

Tabla 3.1: Advancing and receding contact angles of naphthenic and asphaltic bitumen films measured with captive bubble at pH2 and pH12.

pH	Naphthenic bitumen		Asphaltic bitumen	
	ACA ($^{\circ}$)	RCA ($^{\circ}$)	ACA ($^{\circ}$)	RCA ($^{\circ}$)
2	105.3 \pm 1.5	52 \pm 5	112.0 \pm 2.2	88 \pm 3
12	101 \pm 6	43 \pm 6	108.0 \pm 2.1	69.5 \pm 2.3

3.1.3 Electrical state of bitumen-in-water dispersion

In Figure 3.2, we plot the electrophoretic mobility in terms of pH for naphthenic bitumen dispersion at different calcium ion concentrations. The mobility (electrical charge) decreases as pH. The isoelectric point is located at pH \approx 4. The bitumen particles behave as anionic for pH $>$ 4 (64). At low pH, the cationic surfactants on the bitumen surface are protonated to generate cationic sites (RNH_3^+). At pH4, the surface density of amines agrees with the surface density of carboxyl groups. At high pH, the dissociated carboxylate anions ($RCOO^-$) dominate the bitumen surface. With the addition of calcium ions, the specific adsorption of calcium ions at the bitumen surface leading to calcium naphthenates decreases the net electrical charge. There is a "bridging" effect of the divalent cations: chemical binding between surface carboxylate anions of a bitumen particle and calcium ions adsorbed at another bitumen particle or even between neighboring carboxylate groups of the same bitumen particle.

From pH12, the density of calcium naphthenates is greater and the bitumen electrical charge is rapidly neutralized, even the lower electrophoretic mobility points out to the incipient coalescence of the bitumen dispersion.

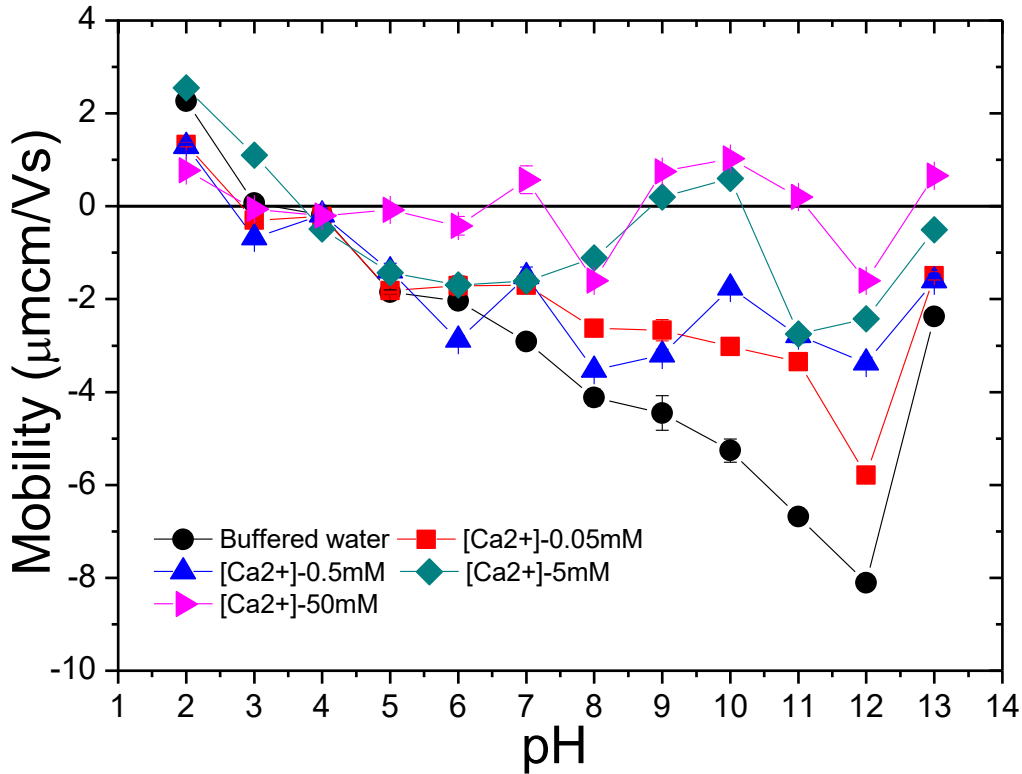


Figure 3.2: Electrophoretic mobility of naphthenic bitumen in terms of pH, for different calcium ion concentrations.

3.1.4 Bitumen-water interfacial tension

Bitumen interface usually requires a certain time to stabilize in water. When a bitumen drop is immersed in an aqueous phase, the interface is reorganized with polar molecules adsorbed onto it. The stabilization time may vary as pH, salt concentration or the thermal history of bitumen. Our fresh naphthenic bitumen needed roughly 200 s to stabilize in water once reached the thermal equilibrium ((see Figure A.2)). In Figure 3.3, we show the equilibrium values of interfacial tension of naphthenic and asphaltic bitumens in basic water (pH 11) in terms of temperature. The interfacial tension of naphthenic bitumen nearly decreases as the temperature and it reaches a value of 4.3 ± 0.3 mN/m at 100°C. In Figure 3.4, we illustrate the variation of naphthenic bitumen drop shape when the surrounding phase was air or water. For the naphthenic bitumen, we found values of interfacial tension much lower than for the asphaltic one. This can be explained by the thermo-activated migration towards the bitumen-water interface of the endogenous surface-active molecules (such as naphthenic acids). Under alkaline conditions, the ionization of naphthenic acids was completely favored.

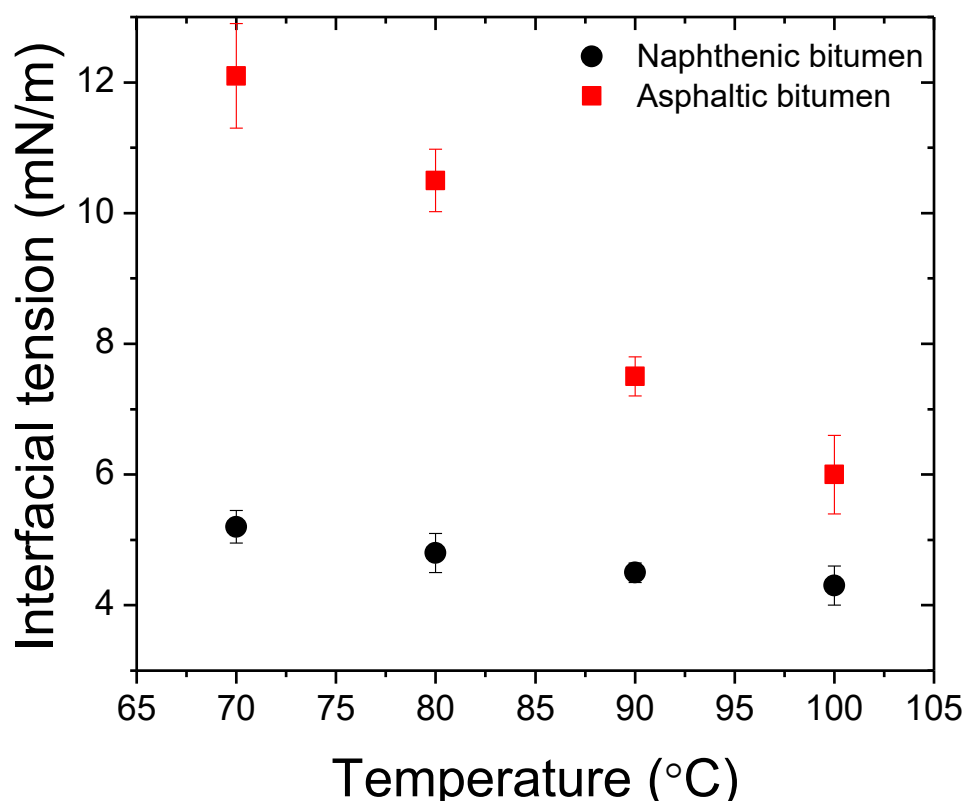


Figure 3.3: Interfacial tension of naphthenic and asphaltic bitumens in water (pH=11), in terms of temperature.

3.1.5 Effect of pH on the bitumen-water interfacial tension

Figure 3.5 shows the interfacial tension of naphthenic bitumen as the pH was changed from 2 to 11. At pH 12, the interfacial tension was ultra low, then it was impossible to form a pendant drop. The interfacial tension varied from 15.2 up to 4.3 mN/m although with a minimum remarkable. The changes in the interfacial tension revealed the complex interfacial activity of bitumen. Our results for $\text{pH} \geq 6$ are in good agreement with the values reported in literature for the naphthenic bitumen from Venezuela (62). For the pH values in the range 3-5, we found very low values of interfacial tension (0.04 mN/m). Naphthenic acids ($R\text{-COOH}$) and amines ($R\text{-NH}_3$) migrated from the bulk of bitumen towards the drop surface and there they were dissociated with different degree as surface cations NH_4^+ and anions $R\text{-COO}^-$. The neutral or scarcely charged interface (pH3-5) allowed the migration of more species and this produced a further lowering of the interfacial tension. In a previous work (58), we estimated the interfacial energy of naphthenic bitumen at room temperature for different pH values and we found partial agreement with the values of this work. However, in the range pH3-5 we found large differences due to the different molecular diffusion (solid versus liquid). In the range pH8-10, the interfacial tension saturated because the interface was blocked with naphthenates. However, it is remarkable the decrease of interfacial

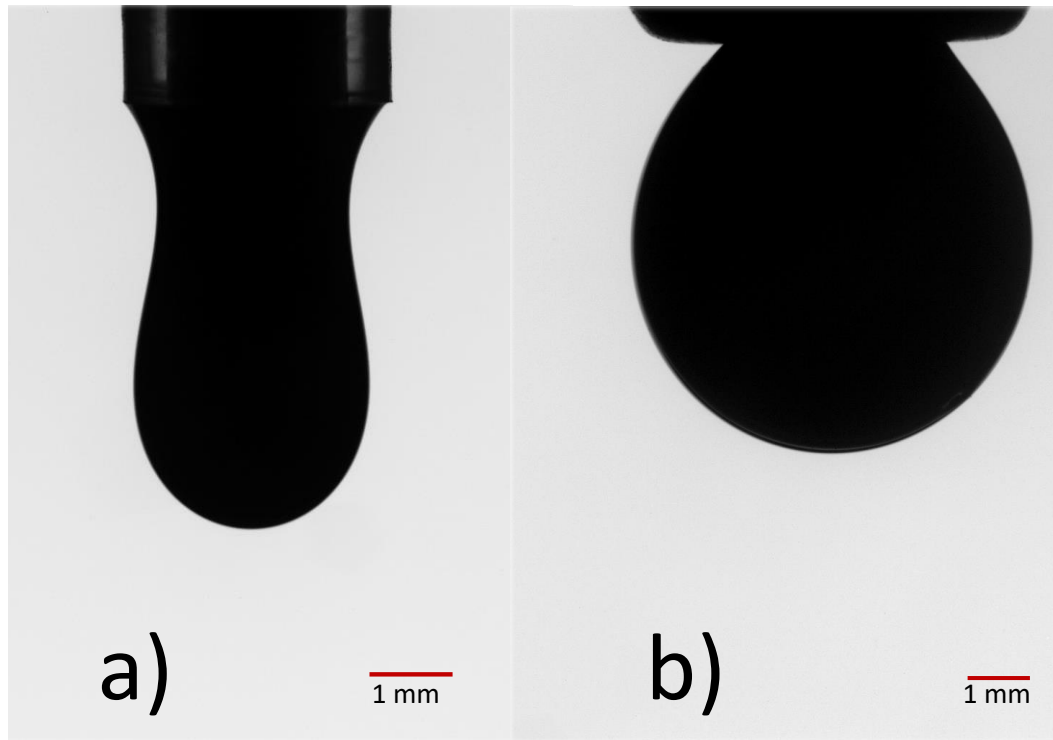


Figure 3.4: Shape of naphthenic bitumen pendant drops at 100° C in (a) air (27.2 mN/m) and (b) water (4.3 mN/m) at pH=11.

tension from pH11 although the net bitumen charge increases (see Figure 3.2). It is known the formation of large and weakly interfacially active asphaltene aggregates in crude oils. The plausible formation of mesostructures or domains rather than a full monolayer onto the interface allowed to unblock the interface (65).

3.1.6 Effect of calcium ions on the bitumen-water interfacial tension

In Table 3.2, we collect the values of interfacial tension of naphthenic bitumen in terms of Ca^{2+} concentration at 100 °C and pH 11. The interfacial tension remained stable below 100mM (5.4 ± 0.3 mN/m) but from it the interfacial tension increased (6.4 ± 0.2 mN/m). This was also observed in a previous work (66). At high pH, the interface film is highly protolysed, which gives rise to strong interactions between the film material and the free Ca^{2+} ions in solution, resulting in the formation of a relatively stable calcium naphthenate film (67). The film of calcium naphthenates has different interfacial properties than pure naphthenic acids.

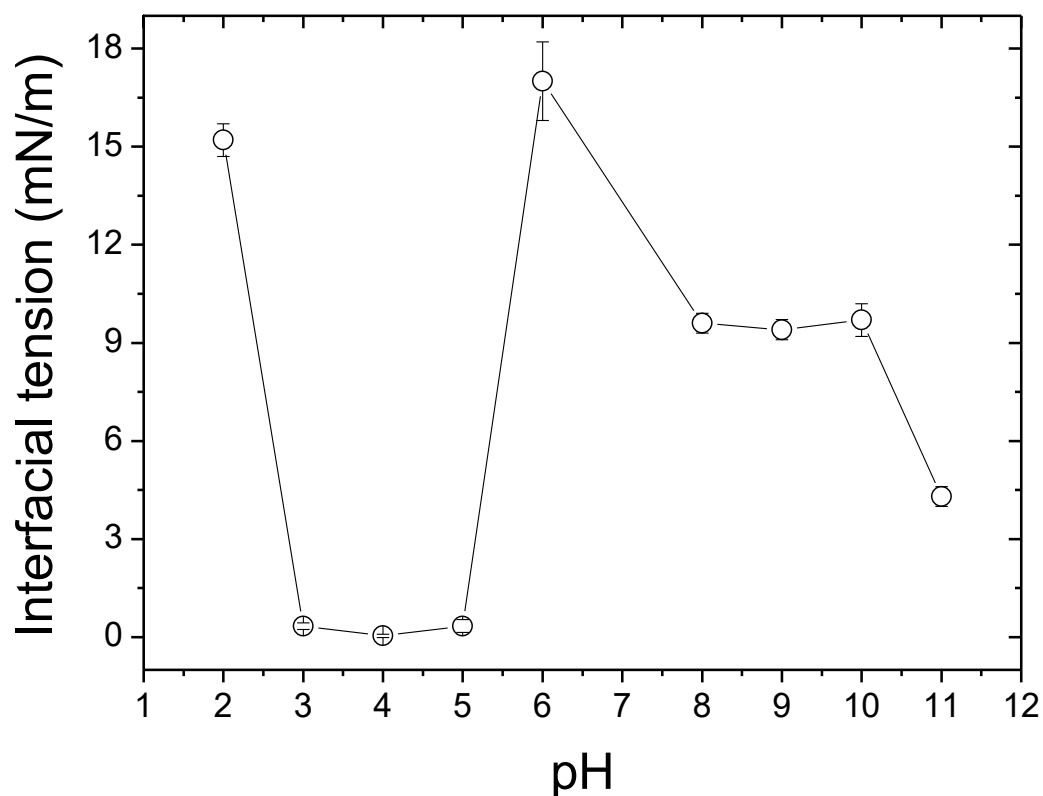


Figure 3.5: Interfacial tension of naphthenic bitumen in terms of pH at 100° C.

3.2 Conclusions

Naphthenic bitumen plays a relevant role in the slurries for paving because the native surfactants can modulate the interfacial behaviour of the bitumen-in-water emulsions. In this work, we performed a detailed interfacial characterization of naphthenic bitumen. The changes in the interfacial tension and wettability in terms of pH revealed the complex interfacial activity of naphthenic bitumen due to its amphiphilic surface chemistry. At pH12, the interfacial tension was ultralow. The surface-active layers (due to the collapse of monolayers) formed by larger molecules dictated the enhanced interfacial and lower electric responses than at pH11. In presence of calcium ions, the fragile balance between electric charge and interfacial tension of bitumen determines its fi-

Tabla 3.2: Interfacial tension of naphthenic bitumen for different calcium ion concentrations at 100° C and pH=11

[Ca ²⁺] (mM)	Interfacial tension (mN/m)
0	5.8 ±0.3
10	5.5 ±0.3
50	5.4 ±0.2
100	6.4 ±0.2

nal response. Above a critical value of calcium content, the formation of calcium naphthenates increased the bitumen interfacial tension, reducing the characteristic relaxation time of bitumen. The uncharged or scarcely charged bitumen (pH3-5) revealed very low values of interfacial tension at high temperature. However, we expect that, at room temperature and in presence of calcium ions, these values will be greater. In addition to interfacial tension, the bitumen behaviour should be further evaluated in terms of interfacial dilational elasticity.

Bitumen spreading on calcareous aggregates at high temperatures

In this chapter, we designed a high temperature goniometer to measure the contact angle of liquid bitumen on mineral aggregate substrates. The drop deposition was conducted once the thermal equilibrium between liquid bitumen and aggregate was attained. We monitored the spreading of sessile drops of viscous naphthenic bitumen and asphaltic bitumen on polished sheets of calcareous aggregates at high temperature (70-100°C). A near complete wetting with very low contact angles (13-24°) was reproduced regardless of the bitumen origin and temperature. Furthermore, the coating degree of the naphthenic and asphaltic bitumens on the calcareous aggregates at high temperature was apparently similar. We found that the bitumen-aggregate adhesion is adequately described by dynamic spreading rather than by equilibrium wettability. Spreading kinetics was ruled by the particular properties of each bitumen such as viscosity and acid index. We found evidences of acid etching of the naphthenic bitumen on the calcareous aggregates during spreading at high temperature.

4.1 Results and discussion

4.1.1 Bitumen surface tension

In Figure 4.1 we show the results of bitumen surface tension in terms of temperature. The well-established linear dependence of surface tension on temperature is confirmed from the corresponding values of squared correlation coefficient: $r^2 = 0.99587$, $r^2 = 0.99034$ and $r^2 = 0.99239$, for each data set. Taking into account the error bars, no significant differences are found between types of bitumen and the measuring methods used, even at 100°C the surface tension agrees. However, we observe statistically different slopes for each bitumen and measuring method. The decreasing rate of surface tension for the naphthenic bitumen measured with the sessile drop method is the highest one whereas with the pendant drop method is the lowest one. The surface tension of the asphaltic bitumen measured with the sessile drop method decreases at an intermediate rate. These results can be explained by the reaction of the acidic surfactants of the naphthenic bitumen with calcite. This could decrease the amount of native surfactants available for liquid-vapor adsorption in the sessile drop. This decrease seems to be lower for the asphaltic bitumen due to its lower acid content and less reactivity with the substrate. In the pendant drop (without contact with substrate), the native surfactants of the naphthenic bitumen saturated the liquid-vapor interface leading to a maximum decrease of the surface tension.

4.1.2 Bitumen spreading

In Figure 4.2, we plot the contact radius normalized by the initial drop volume in terms of time for the naphthenic and asphaltic bitumens. We identified two regimes for the bitumen spreading: first, the viscous regime and then the capillary-adhesive regime (61). Throughout the whole experiment, the bitumen surface tension remained stable. In the viscous regime, higher and faster spreading is expected to occur as lower viscosity (higher temperature). This is confirmed with the asphaltic bitumen. However, although the slow spreading of naphthenic bitumen with moving contact lines for, at least, 2.8h, might be explained by viscosity, an anomalous contact line dynamics was reproduced above 80°C. Further, during the capillary regime, the sessile drops of asphaltic bitumen always reached an equilibrium configuration with static contact lines and with increasing contact radii as temperature. This was not observed for the naphthenic bitumen at similar time scale (10^4 s). However, the slow spreading of naphthenic bitumen also finished with the formation of a thin film over the aggregate substrate.

The contact angles of the naphthenic and asphaltic bitumens on the limestone substrates are shown in Figure 4.3. Just after the drop deposition, the restoring surface tension and viscous force opposed the effect of gravity on the bitumen drop. Due to this, the initial contact angle of

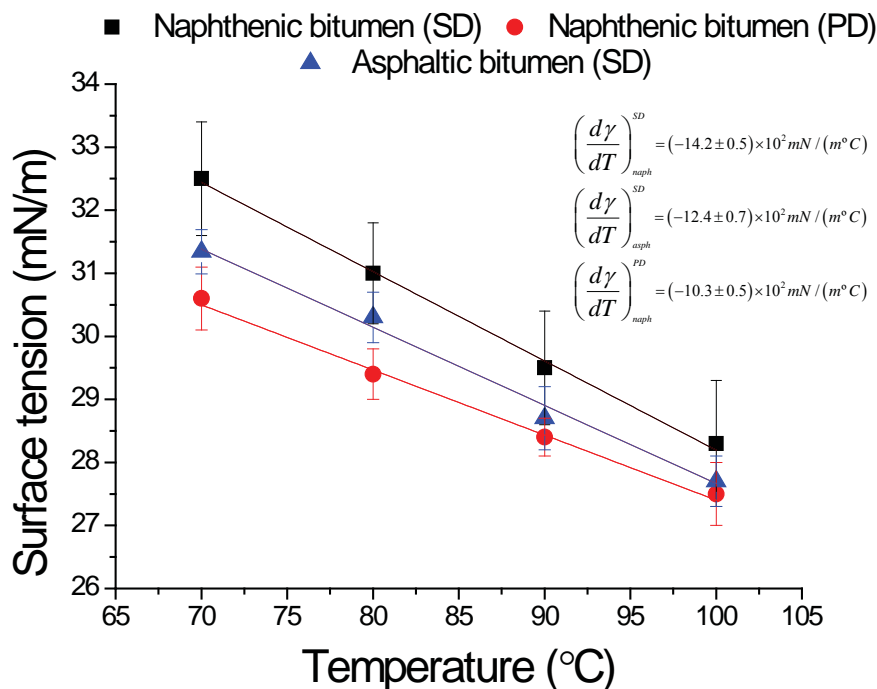


Figure 4.1: Surface tension of the naphthenic and asphaltic bitumens in terms of temperature measured with the sessile drop method (SD). To validate the reliability of the high temperature goniometer, the surface tension of the naphthenic bitumen was also measured with the pendant drop method (PD).

the viscous naphthenic bitumen was lower than 100° . Otherwise, the initial contact angle of the asphaltic bitumen was higher than 100° . The bitumen contact angle decreased as time although at different rates as the temperature was changed. As expected, the asphaltic bitumen began to spread faster than the naphthenic bitumen at the same temperature. Above 90°C , the spreading of both bitumens occurred very rapidly. The crossover in the decreasing rate of contact angle for each temperature points out to the viscous-to-capillary transition in the bitumen spreading. Unlike the asphaltic bitumen, the contact angle of the naphthenic bitumen was continuously decreasing as the drop spreading. Due to this, the viscous-to-capillary transition for the naphthenic bitumen was less clear. However, this transition took longer ($\approx 700\text{s}$) for the naphthenic bitumen than for the asphaltic bitumen ($\approx 350\text{s}$). For both bitumens, the final contact angle reached low values as the temperature increased but only the final contact angle of asphaltic bitumen was stable.

We also monitored the drop volume during the spreading of naphthenic and asphaltic bitumens at different temperatures. For both bitumens, we observed that the volume mostly remained constant, although it decreased ($\leq 20\%$) when the contact angle reached low values ($\theta \leq 40^\circ$) because of numerical artifacts of the ADSA-P algorithm. However, a significant decrease of volume, even for higher values of contact angle, was observed with the naphthenic bitumen at 100°C . Discarding the unlikely significant evaporation of bitumen, this points out to a plausible

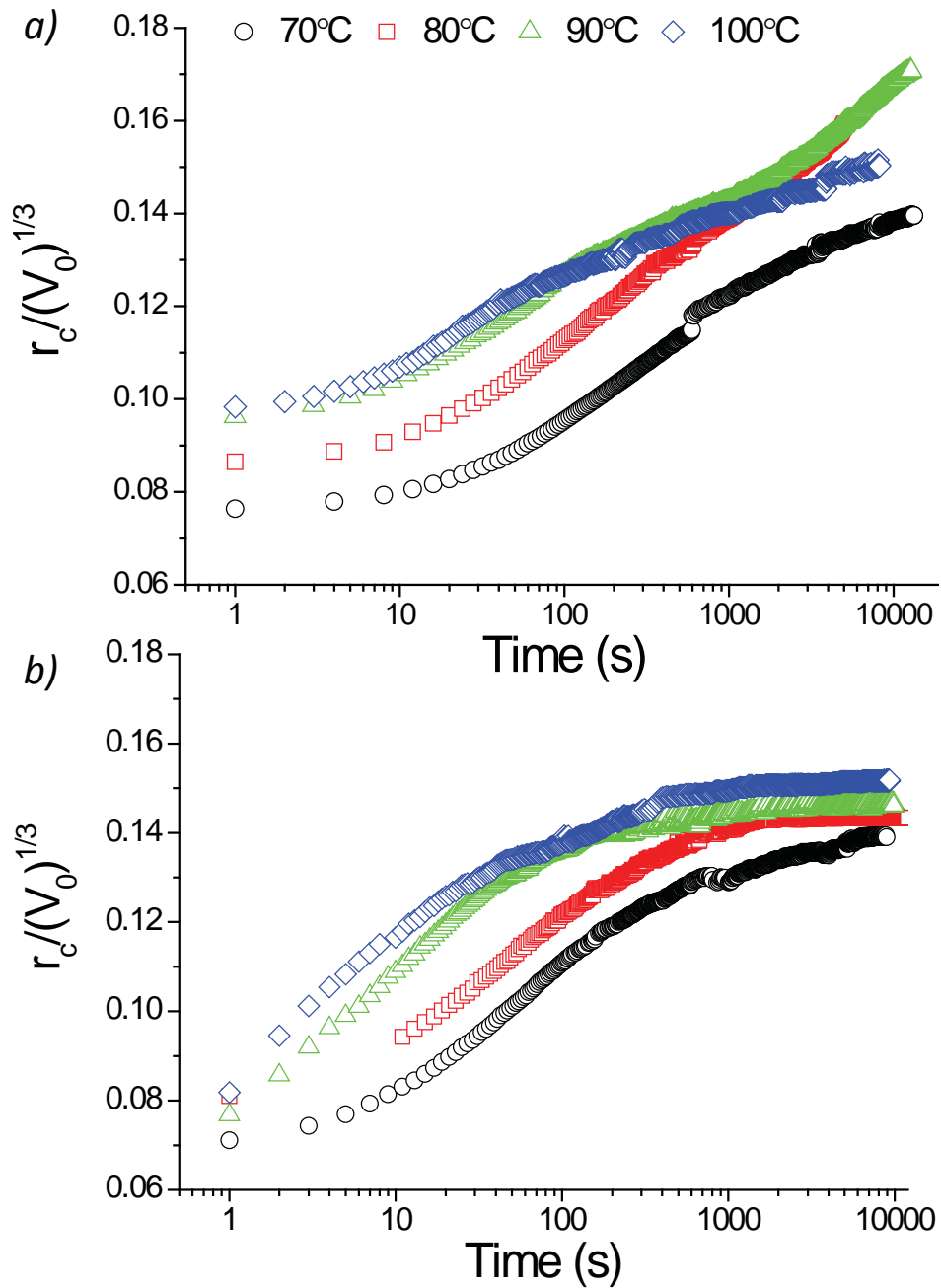


Figure 4.2: Dimensionless contact radius of sessile drops of (a) naphthenic and (b) asphaltic bitumens normalized by the initial drop volume on limestone substrates in terms of time. These values correspond to two single drop experiments accordingly, and the error bars represent the numerical uncertainty of ADSA-P.

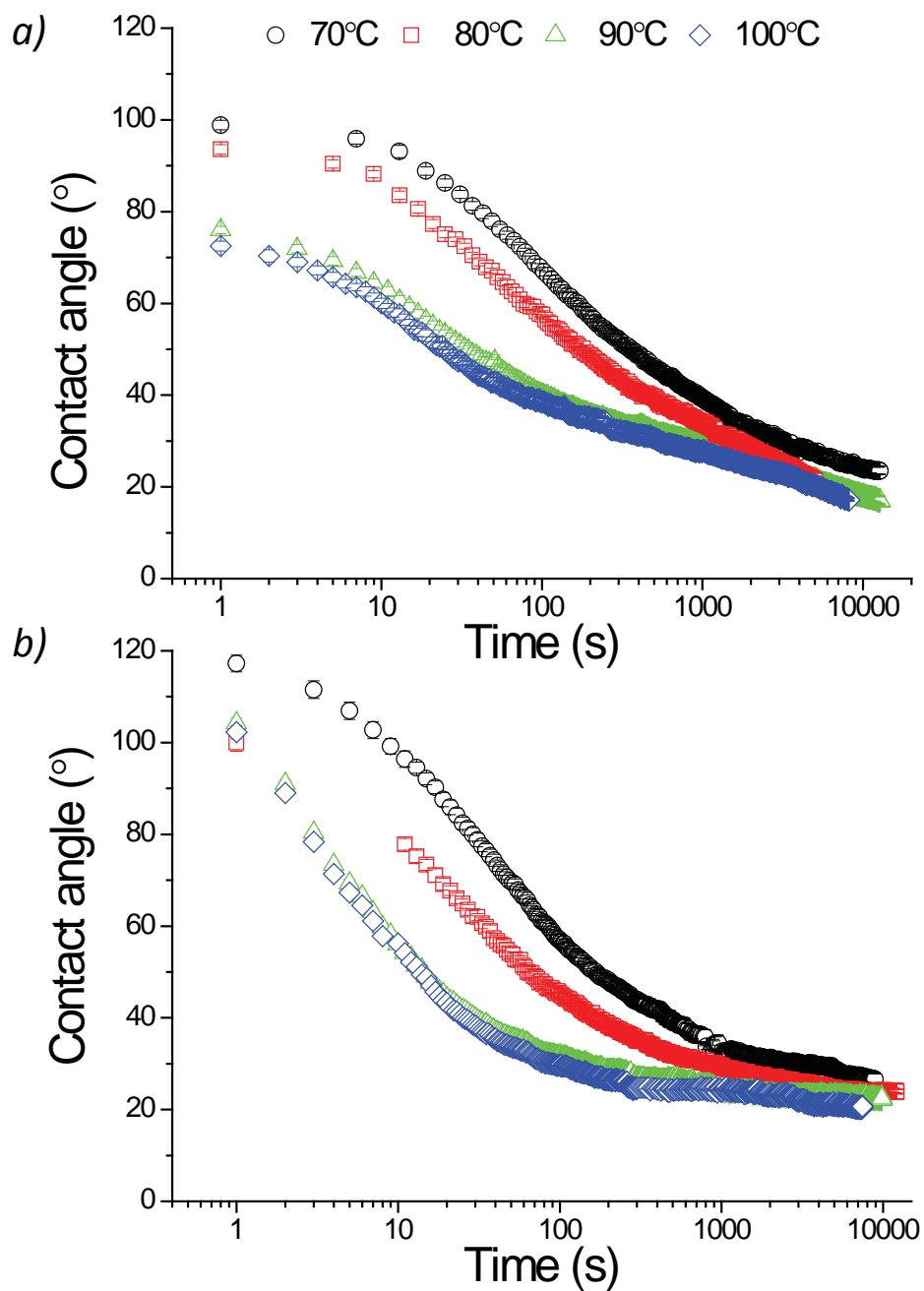


Figure 4.3: Contact angle of (a) naphthenic and (b) asphaltic bitumens on limestone substrates in terms of time. The final contact angle was about 15-20° because of the limitations of ADSA-P. These values correspond to two single drop experiments accordingly, and the error bars represent the numerical uncertainty of ADSA-P.

penetration of bitumen into the mineral surface through its asperities.

4.1.3 Bitumen films

Regardless of the bitumen properties at high temperature (viscosity, surface tension), the naphthenic and asphaltic bitumens formed continuous thin films on the limestone sheets. The features of each bitumen film are collected in Table 4.1. The dimensionless film radius agreed for both bitumens within the range 0.14 – 0.17. This agreement might predict a similar coverage degree. However, the dimensionless thickness (and contact angle) of the naphthenic bitumen film decreased as temperature whereas for the asphaltic bitumen it remained constant above 80°C. The apparent decrease of film thickness for the naphthenic bitumen agrees with the apparent decrease of drop volume mentioned in the former section. This reveals the penetration of the naphthenic bitumen into the limestone aggregate.

Tabla 4.1: Final film height normalized by the initial drop volume, film contact angle and bitumen radius normalized by the initial drop volume for the naphthenic and asphaltic bitumens at different temperatures.

Temperature (°C)	Naphthenic			Asphaltic		
	$h_f/V_0^{1/3}$	$\theta_f(^{\circ})$	$r_f/V_0^{1/3}$	$h_f/V_0^{1/3}$	$\theta_f(^{\circ})$	$r_f/V_0^{1/3}$
70	0.24	21	0.14	0.26	24	0.14
80	0.19	18	0.16	0.21	21	0.14
90	0.17	15	0.17	0.21	21	0.15
100	0.14	13	0.15	0.21	21	0.15

4.1.4 Cross-sectioned calcareous aggregates

After the experiments of drop spreading, some samples were cross sectioned to study the effect of each bitumen into the calcareous aggregates (see Figure 4.4). Only with the naphthenic bitumen at 90°C and 100°C, a gradual penetration of bitumen into the porous aggregate was confirmed.

To further examine the effect of the naphthenic bitumen on the calcareous aggregate surface, we carefully removed the solid bitumen film from the mineral substrates by immersion in a nonpolar solvent (LEYCO-SOL BI) for a few minutes. Then, the substrates were rinsed with the solvent and dried at room temperature. No bitumen trace was observed on the clean substrates. Next, we analyzed the topography of the aggregate substrate by WLCM (see Figure 4.5) and we found that the roughness decreased after the bitumen spreading. This was not observed with blank substrates (without bitumen) after cleaning with the solvent. Moreover, the asphaltic bitumen produced no roughness decrease (not shown).

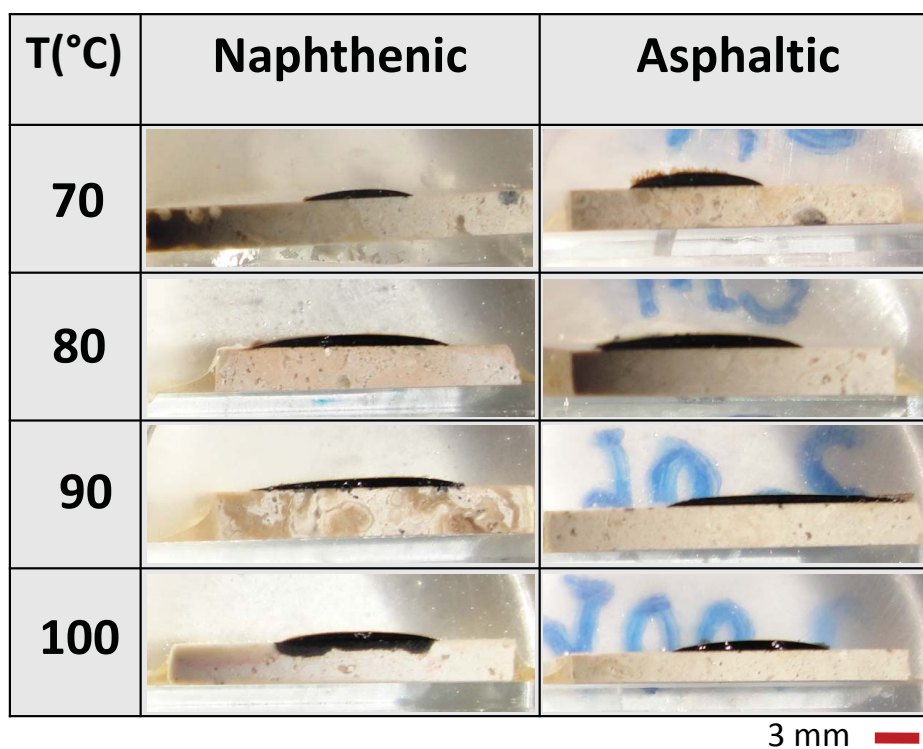


Figure 4.4: Optical images of cross-sectioned calcareous aggregates after spreading of the naphthenic and asphaltic bitumens at different temperatures.

The bitumen absorption becomes significant when the porosity and roughness of the limestone substrate increase because the acid etching produced by the own bitumen at high temperature. The endogenous naphthenic acids of the bitumen reacted with the mineral calcite and in consequence, the surface roughness increased and likely the surface porosity as well. The good adhesion between naphthenic bitumen and calcareous aggregates is twofold motivated by the acidic groups of the natural surfactants of the naphthenic bitumen. Calcite interacts with these functional groups of the bitumen to form stable complexes at the interface and further, the roughness increase improves the micro-mechanical interlocking between bitumen and aggregate.

4.2 Conclusions

We were able to monitor the spreading at high temperature (70-100°C) of bitumen sessile drops deposited on polished mineral aggregates under thermal equilibrium. After spreading, bitumen always reached an equilibrium configuration of pancake-drop or film rather than sessile drop (curved interface). A near complete wetting with very low contact angles (13-24°) was observed regardless of the bitumen origin. Furthermore, the coating degree of the naphthenic and asphaltic bitumens on smooth calcareous aggregates at high temperature was apparently similar. This

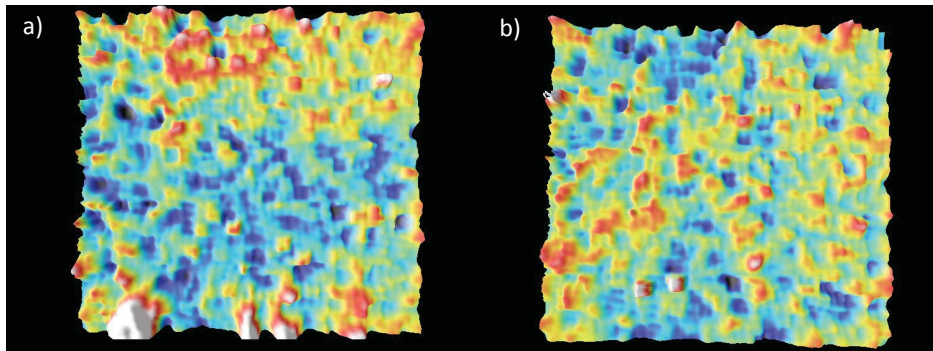


Figure 4.5: WLCM images of the calcareous substrates (scan size area: $5.0 \times 4.7 \text{ mm}^2$) a) before spreading of naphthenic bitumen: $R_q = 1.40 \pm 0.06 \mu\text{m}$ and $R_a = 0.86 \pm 0.08 \mu\text{m}$ and b) after spreading of naphthenic bitumen (without bitumen): $R_q = 0.80 \pm 0.03 \mu\text{m}$ and $R_a = 0.50 \pm 0.06 \mu\text{m}$. These results correspond to the same location approximately.

cannot cancel any thermodynamic framework to quantify the bitumen-aggregate adhesion in hot or warm asphalt mixes. However, spreading kinetics was ruled by the particular properties of each bitumen such as viscosity and acid index. Roughness of high-energy solid surfaces such as mineral aggregates will decrease the spreading rate (advancing front) but will enhance the resistance against the bitumen displacement (receding front).

The naphthenic bitumen produced acid etching on the calcareous aggregates at 100°C . This scenario was validated with the unexpected higher values of bitumen surface tension measured with sessile drops than with pendant drops, the slower viscous-to-capillary transition for the spreading of the naphthenic bitumen, the significant loss of bitumen drop volume, the decreasing thickness of final bitumen film, the small but observable penetration of bitumen into the substrates and the decrease of roughness after bitumen spreading.

Summary and Conclusions

In this thesis, we propose a methodology to evaluate the bitumen-water equilibrium interfacial energy at room temperature. Unlike the pendant drop method for bitumen-water interfacial tension measurements at high temperature, our strategy is appropriate for systems with vanishing density differences and with a very slow interfacial relaxation (high viscosity, low interfacial tension). Further, we avoided the bitumen dilution (eventual traces of solvent), the use of probe liquids for contact angle measurements (mutual solubility with bitumen) and of theories for surface energy calculation (polar-disperse components of surface tension, equation of state). The low-rate dynamic contact angle technique was successfully applied to raw (solvent-free) bitumen films for contact angle hysteresis measurements. Receding contact angles revealed the acid-base properties of naphthenic bitumen. We estimated the bitumen interfacial energy in aqueous medium from the Young equation using the average contact angle of the advancing and receding contact angles for different pH values. The naphthenic bitumen showed high interfacial activity in alkaline aqueous medium (above pH 9) with maximum electrical state and minimum interfacial energy at pH=12. This confirms the self-emulsifiable character of naphthenic bitumen in basic water.

We performed a detailed interfacial characterization of the naphthenic bitumen-water interface. The changes in the interfacial tension and wettability in terms of pH revealed the complex interfacial activity of naphthenic bitumen due to its amphiphilic surface chemistry. At pH12, the

interfacial tension was ultralow. The surface-active layers (due to the collapse of monolayers) formed by larger molecules dictated the enhanced interfacial and lower electric responses than at pH11. In presence of calcium ions, the fragile balance between electric charge and interfacial tension of bitumen determines its final response. Above a critical value of calcium content, the formation of calcium naphthenates increased the bitumen interfacial tension, reducing the characteristic relaxation time of bitumen. The uncharged or scarcely charged bitumen (pH3-5) revealed very low values of interfacial tension at high temperature. However, we expect that, at room temperature and in presence of calcium ions, these values will be greater. In addition to interfacial tension, the bitumen behaviour should be further evaluated in terms of interfacial dilational elasticity.

We were able to monitor the spreading at high temperature (70-100°C) of bitumen sessile drops deposited on polished mineral aggregates under thermal equilibrium. After spreading, bitumen always reached an equilibrium configuration of pancake-drop or film rather than sessile drop (curved interface). A near complete wetting with very low contact angles (13-24°) was observed regardless of the bitumen origin. Furthermore, the coating degree of the naphthenic and asphaltic bitumens on smooth calcareous aggregates at high temperature was apparently similar. This cancels any thermodynamic framework to quantify the bitumen-aggregate adhesion in hot or warm asphalt mixes. However, spreading kinetics was ruled by the particular properties of each bitumen such as viscosity and acid index. Roughness of high-energy solid surfaces such as mineral aggregates will decrease the spreading rate (advancing front) but will enhance the resistance against the bitumen displacement (receding front).

The naphthenic bitumen produced acid etching on the calcareous aggregates at 100°C. This scenario was validated with the unexpected higher values of bitumen surface tension measured with sessile drops than with pendant drops, the slower viscous-to-capillary transition for the spreading of the naphthenic bitumen, the significant loss of bitumen drop volume, the decreasing thickness of final bitumen film, the small but observable penetration of bitumen into the substrates and the decrease of roughness after bitumen spreading.

We are aware that the breaking process of a cationic bitumen emulsion happens under conditions different to the conditions of our interfacial experiments:

- In an emulsion, there are commercial surfactants that can compete with the native surfactants of bitumen.
- The water pH increases, due to the contact with limestone aggregates/filler (the most chemically active aggregate), from 2 to 6 (38)
- The micrometric particles of a bitumen emulsion, instead of millimeter-sized drops, need much lower shape relaxation time ($\frac{\eta R}{\gamma}$).

- The bitumen viscosity at room temperature is much greater (1000 times-see Figure 5.1) than at 100° C and this counterbalances the former decrease in shape relaxation time.
- At room temperature and certain content of calcium ions, the interfacial tension at pH6 is greater and finally the relaxation time becomes lower.

We postulate, from our findings, that a moderate increase in pH and a critical content of calcium ions lead to a weak colloidal stability. Once the emulsion coalescence begins at a moderate rate, the fusion between bitumen particles is controlled by the interfacial tension. This might explain the complete phase separation observed with the naphthenic bitumen in slurry applications.

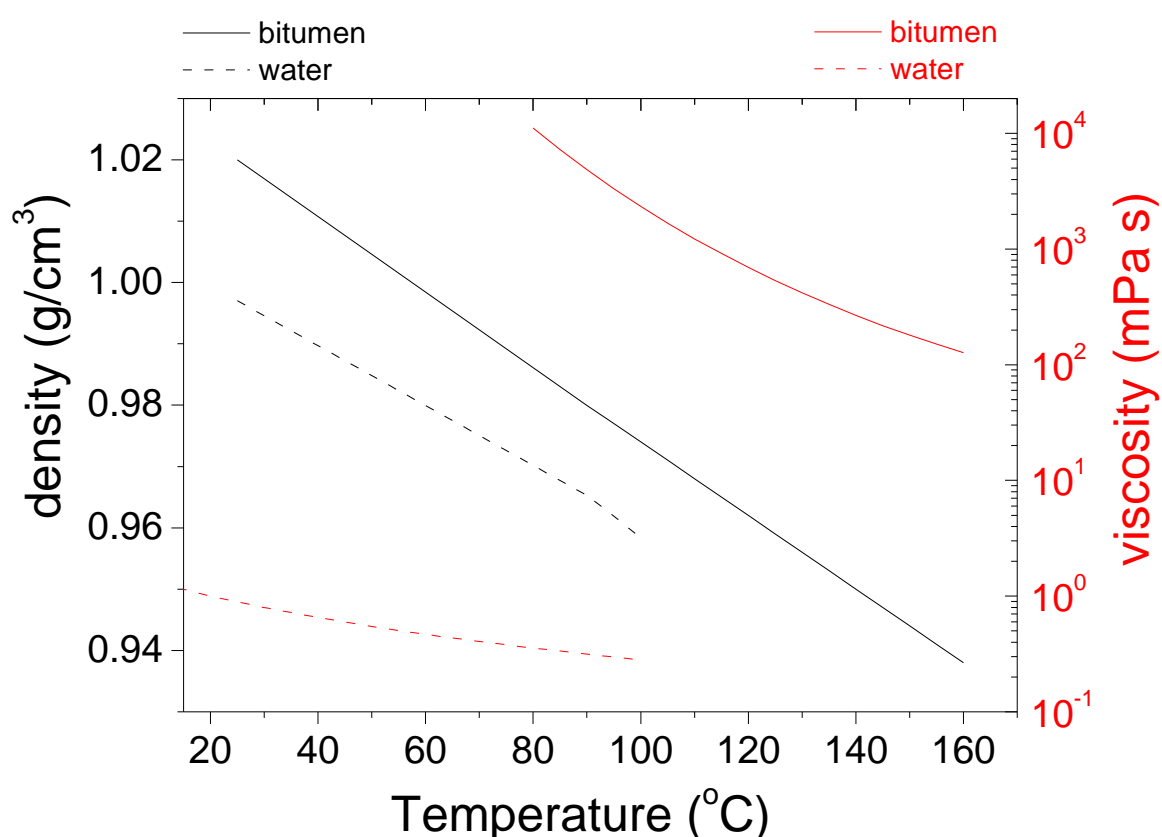


Figure 5.1: Curves for the density and viscosity in terms of temperature for the naphthenic bitumen used in this work. The discontinued lines correspond to water

Finally, we conducted an illustrative experiment where 30 μ l-drops of bitumen dispersions, as prepared in Section 2.3, were placed on polished sheets of limestone aggregates. The different morphology of the stains after drying reveals an exciting scenario: a deposit of particles at the drop edge (pH4), a continuous black deposit (pH5) and a central deposit (pH12 see Figure 5.2). It is known that, unlike the uncharged particles (pH4), the charged particles (pH12) diffuse towards the center of the drop during evaporation (68, 69). The similar brown colour of the stains at pH4 and pH12 reveals an unresolved breaking produced by a fast coalescence or the loss of water

(imbibition and evaporation), respectively. However, at pH5, the stain is a film of black colour. These results are supported by the observation of the different stability of the bitumen dispersion (see Figure 5.2). At 5 mM of calcium ion content, the dispersion is still stable (regardless of the visible creaming and settling) at pH12 but the dispersion instability is different between pH4 and pH5 as happens with the stain morphology. The visible floccules of bitumen adhered to the tube wall at pH5 point out to that large and positively charged clusters, produced after slow

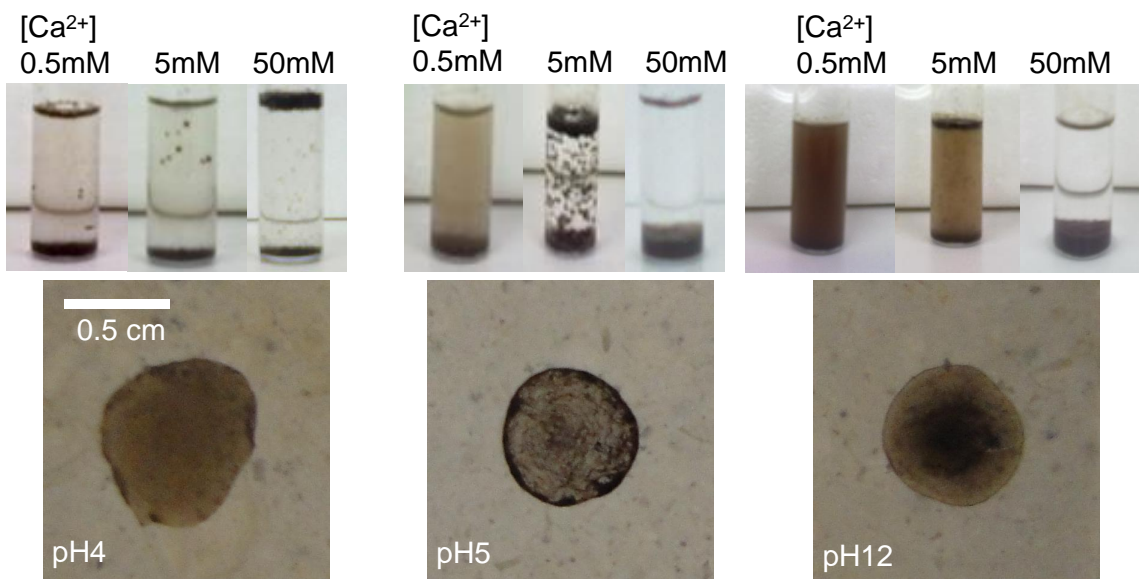


Figure 5.2: Glass tubes with bitumen dispersions at pH4, 5 and 12 and different calcium content (0.5, 5 and 50 mM), and top-view images of the stains formed on limestone aggregates after drying of the bitumen dispersions at pH4, 5 and 12.

Supplementary data

A.1 High-temperature chamber for interfacial/surface tension measurements of heavy bitumen

In Figure [A.1](#), we show the dimensions and details of the aluminium chamber designed to measure surface and interfacial tensions with bitumen pendant drops at high temperature.

A.2 Stability of bitumen-water interfacial tension

In Figure [A.2](#), we plot the bitumen-water interfacial tension in terms of time at at 100° C and pH9 to illustrate the decay time. We observe that the interfacial tension took, on average, about 200s to stabilize. After, the interfacial tension value remained stable for 800s.

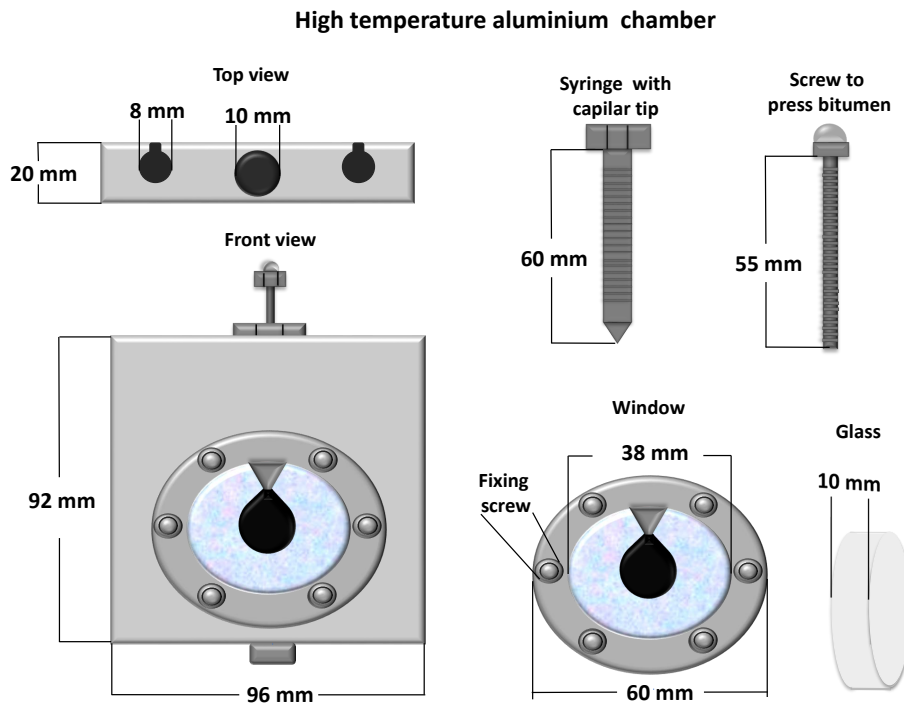


Figure A.1: Scheme of chamber

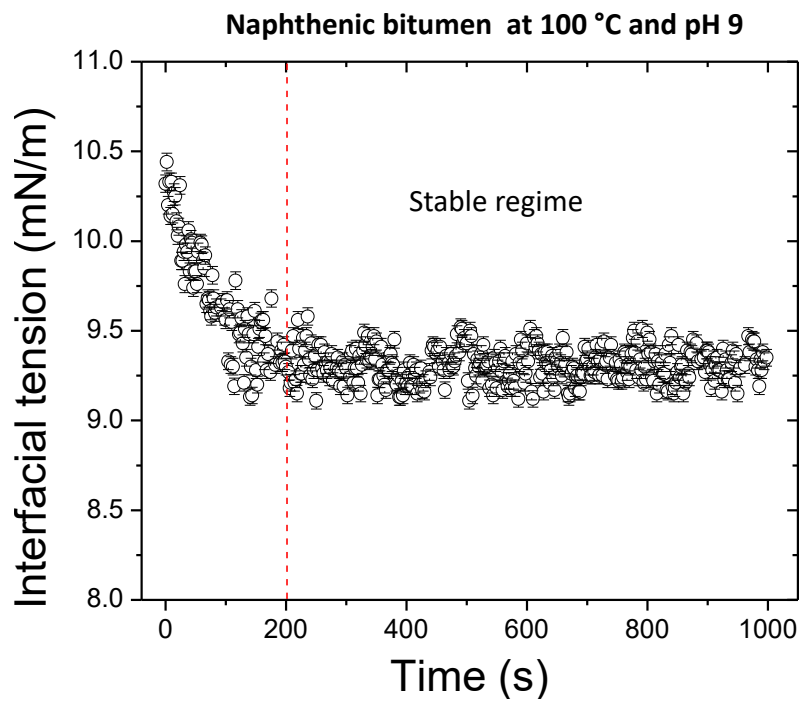


Figure A.2: Interfacial tension of naphthenic bitumen in terms of time (at 100° C and pH9)

A.3 Rigid skin

Under certain circumstances, such as aging by continued thermo-oxidation, asphaltenes can adsorb at the bitumen-water interface in the form of aggregates and the interfacial layers become thick. A solid-like skin is formed due to interactions (cross-linking, etc.) of the adsorbed species. The rigid skin prevents the drop deformation of aged bitumen (see Figure A.3).



Figure A.3: Evidence of the elasticity loss of aged naphthenic bitumen. It is clear the spherical tip of the filament adopted after days from the dispensation.

Bibliography

- [1] Carreón Blaine, E. A. Del hule al chapopote en la plástica mexicana. Una revista historiográfica. *Trace* **2016**, 9 – 44.
- [2] Aguilera, C. Algunos datos sobre el chapopote en las fuentes documentales del siglo XVI. *Estudios de Cultura Náhuatl* **1980**, 4, 335–343.
- [3] Lesueur, D. The colloidal structure of bitumen: Consequences on the rheology and on the mechanisms of bitumen modification. *Advances in Colloid and Interface Science* **2009**, 145, 42 – 82.
- [4] Jager, A.; Lackner, R.; Eisenmenger-Sittner, C.; Blab, R. Identification of four material phases in bitumen by atomic force microscopy. *Road Materials and Pavement Design* **2004**, 5, 9–24.
- [5] Redelius, P. Asphaltenes in bitumen, what they are and what they are not. *Road Materials and Pavement Design* **2009**, 10, 25–43.
- [6] Sjoblom, J. *Encyclopedic Handbook of Emulsion Technology*; CRC Press, 2001.
- [7] Lesueur, D.; Uguet, N.; Hurtado, J.; Herrero, L. Nanoemulsiones de betún. *Carreteras: Revista técnica de la Asociación Española de la Carretera* **2009**, 33–46.
- [8] Simoes, D.; Almeida-Costa, A.; Benta, A. Preventive maintenance of road pavement with microsurfacing: An economic and sustainable strategy. *International Journal of Sustainable Transportation* **2017**, In press. DOI: 10.1080/15568318.2017.1302023.

- [9] Nellensteyn, F.; Roodenburg, N. Surface tension-temperature curves of asphalt bitumen and similar products. **1930**,
- [10] Moraes, R.; Velasquez, R.; Bahia, H. Measuring the effect of moisture on asphalt-aggregate bond with the bitumen bond strength test. *Transportation Research Record: Journal of the Transportation Research Board* **2011**, 70–81.
- [11] Ziyani, L.; Gaudefroy, V.; Ferber, V.; Hammoum, F. A predictive and experimental method to assess bitumen emulsion wetting on mineral substrates. *Colloids and Surfaces A: Physicochemical and Engineering Aspects* **2016**, 489, 322–335.
- [12] Khan, A.; Redelius, P.; Kringos, N. Evaluation of adhesive properties of mineral-bitumen interfaces in cold asphalt mixtures. *Construction and Building Materials* **2016**, 125, 1005–1021.
- [13] Fischer, H. R.; Dillingh, E.; Hermse, C. On the interfacial interaction between bituminous binders and mineral surfaces as present in asphalt mixtures. *Applied Surface Science* **2013**, 265, 495–499.
- [14] Di Lorenzo, M.; Vinagre, H.; Joseph, D. Adsorption of Intan-100 at the bitumen/aqueous solution interface studied by spinning drop tensiometry. *Colloids and Surfaces A: Physicochemical and Engineering Aspects* **2001**, 180, 121–130.
- [15] Chaverot, P.; Cagna, A.; Glita, S.; Rondelez, F. Interfacial tension of bitumen- water interfaces. Part 1: Influence of endogenous surfactants at acidic pH. *Energy & Fuels* **2007**, 22, 790–798.
- [16] Lesueur, D.; Potti, J. J. Cold mix design: A rational approach based on the current understanding of the breaking of bituminous emulsions. *Road Mater. Pavement* **2004**, 5, 65–87.
- [17] Jada, A.; Salou, M.; Siffert, B. Effects of the bitumen polar fractions on the stability of bitumen aqueous dispersions. *Petrol. Sci. Tech.* **2001**, 19, 119–127.
- [18] Boulange, L.; Sterczynskia, F. Study of Interfacial Interactions between Bitumen and Various Aggregates Used in Road Construction. *J. Adhes. Sci. Technol.* **2012**, 26, 163–173.
- [19] Acevedo, S.; Méndez, B.; Rojas, A.; Layrissé, I.; Rivas, H. Asphaltenes and resins from the Orinoco basin. *Fuel* **1985**, 64, 1741–1747.
- [20] Takamura, K.; Chow, R. S. The electric properties of the bitumen/water interface. Part II. Application of the ionizable surface-group model. *Colloids and Surfaces* **1985**, 15, 35–48.

-
- [21] Bonakdar, L.; Philip, J.; Bardusco, P.; Petkov, J.; Potti, J.; Mlard, P.; Leal-Calderon, F. Rupturing of bitumen-in-water emulsions: experimental evidence for viscous sintering phenomena. *Colloids and Surfaces A: Physicochemical and Engineering Aspects* **2001**, *176*, 185 – 194.
- [22] Yarranton, H.; Sztukowski, D.; Urrutia, P. Effect of interfacial rheology on model emulsion coalescence: I. Interfacial rheology. *Journal of colloid and interface science* **2007**, *310*, 246–252.
- [23] Boucard, L.; Schmitt, V.; Farcas, F.; Gaudefroy, V. Bitumen emulsions formulation and destabilisation process relationship: influence of salts addition. *Road Materials and Pavement Design* **2015**, *16*, 330–348.
- [24] Strassner, J. Effect of pH on interfacial films and stability of crude oil-water emulsions. *Journal of Petroleum Technology* **1968**, *20*, 303–312.
- [25] Goldszal, A.; Bourrel, M.; Hurtevent, C.; Volle, J. The Third International Conference on Petroleum Phase Behavior and Fouling. *New Orleans, USA* **2002**,
- [26] Drelich, J.; Bukka, K.; Miller, J. D.; Hanson, F. V. Surface Tension of Toluene-Extracted Bitumens from Utah Oil Sands as Determined by Wilhelmy Plate and Contact Angle Techniques. *Energy & Fuels* **1994**, *8*, 700–704.
- [27] Xu, Y. Dynamic Interfacial Tension between Bitumen and Aqueous Sodium Hydroxide Solutions. *Energy & Fuels* **1995**, *9*, 148–154.
- [28] Pandit, A.; Miller, C. A.; Quintero, L. Interfacial tensions between bitumen and aqueous surfactant solutions by maximum bubble pressure technique. *Colloids Surf., A* **1995**, *98*, 35–41.
- [29] Moran, K. Roles of Interfacial Properties on the Stability of Emulsified Bitumen Droplets. *Langmuir* **2007**, *23*, 4167–4177.
- [30] Chaverot, P.; Cagna, A.; Glita, S.; Rondelez, F. Interfacial Tension of Bitumen-Water Interfaces. Part 1: Influence of Endogenous Surfactants at Acidic pH. *Energy & Fuels* **2008**, *22*, 790–798.
- [31] Eckmann, B.; Simaillaud, B.; Verlhac, P.; Van Nieuwenhuyze, K.; Verzaro, F. Measurement and interpretation of the interfacial tension of bitumen. *Revue Generale des Routes et des Aerodromes* **2001**, *797*, 57–63.
- [32] Moran, K.; Yeung, A.; Czarnecki, J.; Masliyah, J. Micron-scale tensiometry for studying density-matched and highly viscous fluids-with application to bitumen-in-water emulsions. *Colloids Surf., A* **2000**, *174*, 147–157.

- [33] Vargha-Butler, E. I.; Potoczny, Z. M.; Zubovits, T. K.; Budziak, C. J.; Neumann, A. W. Surface tension of bitumen from contact angle measurements on films of bitumen. *Energy & Fuels* **1988**, *2*, 653–656.
- [34] Rodriguez-Valverde, M. A.; Cabrerizo-Vilchez, M. A.; Paez-Dueñas, A.; Hidalgo-Alvarez, R. Stability of highly charged particles: bitumen-in-water dispersions. *Colloids Surf., A* **2003**, *222*, 233–251.
- [35] Miknis, F. P.; Pauli, A. T.; Beemer, A.; Wilde, B. Use of NMR imaging to measure interfacial properties of asphalts. *Fuel* **2005**, *84*, 1041–1051.
- [36] Jada, A.; Salou, A. Effects of the asphaltene and resin contents of the bitumens on the water-bitumen interface properties. *J. Pet. Sci. Eng.* **2002**, *33*, 185–193.
- [37] Bagampadde, U.; Isacson, U.; Kiggundu, B. Impact of bitumen and aggregate composition on stripping in bituminous mixtures. *Mater Struct* **2006**, *39*, 303–315.
- [38] Ziyani, L.; Gaudefroy, V.; Ferber, V.; Deneele, D.; Hammoum, F. Chemical reactivity of mineral aggregates in aqueous solution: relationship with bitumen emulsion breaking. *Journal of Materials Science* **2014**, *49*, 2465–2476.
- [39] Somé, S. C.; Gaudefroy, V.; Delaunay, D. Estimation of bonding quality between bitumen and aggregate under asphalt mixture manufacturing condition by thermal contact resistance measurement. *Int. J. Heat Mass Transfer.* **2012**, *55*, 6854–6863.
- [40] Nowell, D.; Powell, M. Determination of adhesion in bitumen-mineral systems by heat-of-immersion calorimetry. *J Therm Anal* **1991**, *37*, 2109–2124.
- [41] Read, J.; Whiteoak, D. *The Shell Bitumen Handbook*; Thomas Telford, 2003.
- [42] Alvarez, A. E.; Ovalles, E.; Caro, S. Assessment of the effect of mineral filler on asphalt-aggregate interfaces based on thermodynamic properties. *Construction and Building Materials* **2012**, *28*, 599–606.
- [43] Young, T. An Essay on the Cohesion of Fluids. *Phil. Trans. R. Soc.* **1805**, *95*, 65–87.
- [44] Hefer, A.; Bhasin, A.; Little, D. Bitumen Surface Energy Characterization Using a Contact Angle Approach. *J. Mater. Civ. Eng.* **2006**, *18*, 759–767.
- [45] Drelich, J.; Miller, J. D. Examination of Neumann's Equation-of-State for Interfacial Tensions. *J. Colloid Interface Sci.* **1994**, *167*, 217–220.
- [46] Rudin, J.; Wasan, D. T. Mechanisms for lowering of interfacial tension in alkali/acidic oil systems 1. Experimental studies. *Colloids and Surfaces* **1992**, *68*, 67–79.

-
- [47] Boulangé, L.; Bonin, E.; Saubot, M. Physicochemical characterisations of the bitumen aggregate interface to get a better understanding of stripping phenomena. *Road Mater Pavement* **2013**, *14*, 384–403.
- [48] Rodríguez-Valverde, M.; Cabrerizo-Vílchez, M.; Rosales-López, P.; Páez-Dueñas, A.; Hidalgo-Alvarez, R. Contact angle measurements on two (wood and stone) non-ideal surfaces. *Colloids and Surfaces A: Physicochemical and Engineering Aspects* **2002**, *206*, 485–495.
- [49] Eustathopoulos, N.; Nicolas, M. G.; Drevet, B. *Wettability at High Temperatures*; Pergamon Materials Series; Pergamon, 1999; Vol. 3; pp 1 – 53.
- [50] Rodríguez-Valverde, M. A.; Montes Ruiz-Cabello, F. J.; Cabrerizo-Vilchez, M. A. A new method for evaluating the most-stable contact angle using mechanical vibration. *Soft Matter* **2011**, *7*, 53–56.
- [51] Moraila-Martinez, C. L.; Montes Ruiz-Cabello, F. J.; Cabrerizo-Vilchez, M. A.; Rodríguez-Valverde, M. A. The effect of contact line dynamics and drop formation on measured values of receding contact angle at very low capillary numbers. *Colloids Surf., A* **2012**, *404*, 63–69.
- [52] Ruiz-Cabello, F. M.; Rodríguez-Valverde, M.; Cabrerizo-Vilchez, M. Contact angle hysteresis on polymer surfaces: an experimental study. *Journal of Adhesion Science and Technology* **2011**, *25*, 2039–2049.
- [53] Noguera-Marín, D.; Moraila-Martínez, C. L.; Cabrerizo-Vílchez, M. A.; Rodríguez-Valverde, M. A. Transition from Stripe-like Patterns to a Particulate Film Using Driven Evaporating Menisci. *Langmuir* **2014**, *30*, 7609–7614.
- [54] Nellensteyn, F.; Roodenburg, N. Die Ausbreitung von Wasser auf Asphaltbitumen und Teer. *Colloid Polym. Sci.* **1933**, *63*, 339–347.
- [55] Neuville, M.; Rondelez, F.; Cagna, A.; Sanchez, M. Two-Step Adsorption of Endogenous Asphaltenic Surfactants at the Bitumen-Water Interface. *Energy & Fuels* **2012**, *26*, 7236–7242.
- [56] Saad, S. M.; Neumann, A. W. Axisymmetric Drop Shape Analysis (ADSA): An Outline. *Advances in Colloid and Interface Science* **2016**, *238*, 62 – 87.
- [57] Rodríguez-Valverde, M. A.; Ramon-Torregrosa, P.; Páez-Dueñas, A.; Cabrerizo-Vílchez, M. A.; Hidalgo-Álvarez, R. Imaging techniques applied to characterize bitumen and bituminous emulsions. *Adv. Colloid Interface Sci.* **2008**, *136*, 93–108.
- [58] Guerrero-Barba, F.; Moraila-Martínez, C. L.; Lesueur, D.; Cabrerizo-Vílchez, M. A.; Rodríguez-Valverde, M. A. Interfacial energy of heavy naphthenic bitumen in aqueous medium. *Fuel* **2013**, *112*, 45–49.

- [59] Dourado, E. R.; Pizzorno, B. S.; Motta, L. M. G.; Simao, R. A.; Leite, L. F. Analysis of asphaltic binders modified with PPA by surface techniques. *J Microsc* **2014**, *254*, 122–128.
- [60] Hefer, A. W.; Little, D. N.; Herbert, B. E. Bitumen surface energy characterization by inverse gas chromatography. *J. Test. Eval.* **2007**, *35*, 233–239.
- [61] Jacobasch, H. J.; Grundke, K.; Schneider, S.; Simon, F. Surface Characterization of Polymers by Physico-Chemical Measurements. *J. Adhesion* **1995**, *48*, 57–73.
- [62] Acevedo, S.; Gutierrez, X.; Rivas, H. Bitumen-in-Water Emulsions Stabilized with Natural Surfactants. *J. Colloid Interface Sci.* **2001**, *242*, 230–238.
- [63] Guerrero-Barba, F.; Cabrerizo-Vílchez, M. A.; Rodríguez-Valverde, M. A. Bitumen spreading on calcareous aggregates at high temperature. *Journal of Materials Science* **2014**, *49*, 7723–7729.
- [64] Rodríguez-Valverde, M.; Cabrerizo-Vílchez, M.; Páez-Dueñas, A.; Hidalgo-Alvarez, R. Stability of highly charged particles: bitumen-in-water dispersions. *Colloids and Surfaces A: Physicochemical and Engineering Aspects* **2003**, *222*, 233–251.
- [65] Kiran, S. K.; Ng, S.; Acosta, E. J. Impact of Asphaltenes and Naphthenic Amphiphiles on the Phase Behavior of Solvent- Bitumen- Water Systems. *Energy & Fuels* **2011**, *25*, 2223–2231.
- [66] Guerrero-Barba, F. I.; Moraila-Martínez, C. L.; Lesueur, D.; Cabrerizo-Vílchez, M. A.; Rodríguez-Valverde, M. A. Interfacial energy of heavy naphthenic bitumen in aqueous medium. *Fuel* **2013**, *112*, 45 – 49.
- [67] Havre, T. E. Formation of calcium naphthenate in water/oil systems, naphthenic acid chemistry and emulsion stability. **2002**, *Doctoral thesis*.
- [68] Noguera-Marin, D.; Moraila-Martinez, C. L.; Cabrerizo-Vilchez, M. A.; Rodriguez-Valverde, M. A. In-plane particle counting at contact lines of evaporating colloidal drops: effect of the particle electric charge. *Soft Matter* **2015**, *11*, 987–993.
- [69] Noguera-Marín, D.; Moraila-Martínez, C. L.; Cabrerizo-Vílchez, M.; Rodríguez-Valverde, M. A. Impact of the collective diffusion of charged nanoparticles in the convective/capillary deposition directed by receding contact lines. *The European Physical Journal E* **2016**, *39*, 20.